

SIMULATION OF GAMMA CAMERA IN YEDITEPE UNIVERSITY HOSPITAL  
WITH GATE

by  
Gülçin İrim

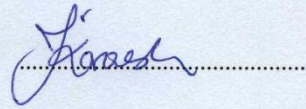
Submitted to the Institute of Graduate Studies in  
Science and Engineering in partial fulfillment of  
the requirements for the degree of  
Master of Science  
in  
Physics Department

Yeditepe University  
2013

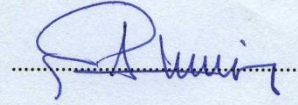
SIMULATION OF GAMMA CAMERA IN YEDITEPE UNIVERSITY  
HOSPITAL WITH GATE

APPROVED BY:

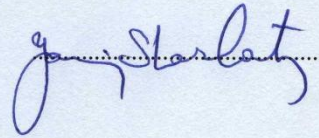
Assoc. Prof. Ş. İpek KARAASLAN  
(Supervisor)



Assoc. Prof. Ertan AKŞAHİN



Prof. Dr. Yani SKARLATOS



DATE OF APPROVAL: 25/06/2013

## **ACKNOWLEDGEMENT**

This thesis arose in mainly of the results of the experiments that have been conducted at Nuclear Medicine Department of Yeditepe University Hospital since it was established.

Foremost, I would like to express my sincere gratitude to my advisor Assoc.Prof. Dr. Ş. İpek KARAASLAN for her continuous support and guidance throughout my MSc study. With her encouragement, her enthusiasm, her inspiration, her immense knowledge and her great efforts to explain things clearly and simply, She made this thesis possible.

Besides, I would also like to thank myfriends and colleague Türkay TOKLU and Didar TALAT for their inexhaustible patience and giving wise advices, helping with various applications. I would like to thank Nuclear Medicine Department Staff for their helping to me.

Finally, I wish to thank my family. They have always supported me. To them I dedicate this thesis.

## **ABSTRACT**

### **SIMULATION OF GAMMA CAMERA IN YEDITEPE UNIVERSITY HOSPITAL WITH GATE**

The aim of this thesis is to have a detail simulation of Gamma Camera in Yeditepe University Hospital Nuclear Medicine Department to carry the personal dosimetric calculations for all the patients before the treatment.

In this thesis, Gamma Camera being used routinely in Yeditepe University Hospital Nuclear Medicine Department was investigated experimentally and with Monte Carlo simulation. A new and open Monte Carlo Code source, GATE, was used that for simulations running commands in C++ language.

First of all various crystals and activities were investigated with the simulations. Secondly, The performance experiments of Gamma Camera (made PHILIPS-forte) in Yeditepe University Hospital were done according to NEMA criteria and also at the same time the simulations were run. Finally, the experimental and simulation results were compared and the new results were all installed to the simulation in order to have the Yeditepe University Hospital Gamma Camera complete simulation.

## ÖZET

### **YEDİTEPE ÜNİVERSİTESİ HASTANESİNE AİT GAMA KAMERA CİHAZININ GATE İLE SİMÜLASYONU**

Bu tezin amacı, Yeditepe Üniversitesi Hastanesi Nükleer Tıp bölümünde bulunan Gama Kamera cihazının ayrıntılı simülasyonunu yaparak tedavi öncesi tüm hastalar için kişisel dozimetrik hesaplamaları yapmak.

Bu tezde, Yeditepe Üniversitesi Hastanesi Nükleer Tıp Bölümünde rutin olarak kullanılan Gama Kamera deneysel ve Monte Carlo simülasyonu ile araştırıldı. Simülasyon için yeni bir Monte Carlo yazılımı olan ve C++ dilinde hazırlanmış. GATE programı tercih edilmiştir.

İlk olarak, Çeşitli kristaller ve aktiviteler ile simülasyon incelenmiştir. İkinci olarak ise, Yeditepe Üniversitesi Hastanesi PHILIPS-forte model Gama Kamera performans kabul testleri deneysel ve simülasyon olarak yapılmıştır. Sonuç olarak deneysel ve simülasyon sonuçları karşılaştırılmıştır. Elde edilen deneysel sonuçlar, simülasyon içine monte edilerek hastanede kullanılan Gama Kameranın birebir aynısı oluşturulmaya çalışılmıştır.

## TABLE OF CONTENTS

PAGE OF APPROVAL .....	ii
ACKNOWLEDGEMENT .....	iii
ABSTRACT .....	iv
ÖZET .....	v
TABLE OF CONTENTS .....	vi
LIST OF FIGURES .....	viii
LIST OF TABLE .....	xi
LIST OF ABBREVIATIONS .....	xii
1. INTRODUCTION .....	1
2. IMAGING IN MEDICINE .....	3
2.1. GENERAL IMAGING CONSIDERATIONS.....	4
2.2. RADIOPHARMACEUTICALS.....	5
2.2.1. The ideal Properties of Radionuclides and Carrier Molecules.....	5
2.2.2. Technetium.....	8
2.3. GAMMA CAMERA COMPONENTS.....	10
2.3.1. Collimator .....	11
2.3.2. Types of Collimators.....	12
2.3.3. Detection by the NaI Crystal.....	13
2.3.4. Optical to Electrical Signal Conversion .....	13
2.3.5. PM Tube Signal Amplification .....	14
2.3.6. Electronic Amplification.....	15
2.3.7. Signal Energy Calibration .....	15
2.3.8. Energy Discrimination .....	15
2.3.9. Energy Measurement.....	15
2.3.10. Gamma Camera Performance .....	16
2.4. NUCLEAR MEDICINE IMAGING .....	17
2.4.1. Multimodality Imaging .....	17
2.5. RADIATION INTERACTIONS .....	19
2.5.1. Photoelectric Effect.....	19
2.5.2. Compton Scattering.....	20
2.5.3. Pair Production.....	22
3. MONTE CARLO SIMULATIONS .....	23

3.1. GATE.....	24
3.1.1. The building GATE of 8 steps .....	25
3.2. ROOT OUTPUT FILE .....	26
4. METHODS & MATERIALS .....	27
4.1. BASIC GAMMA CAMERA SIMULATION .....	27
4.1.1. Various Crystals with Different Thickness and Activities .....	30
4.2. PERFORMANCE OF GAMMA CAMERA ACCEPTANCE TESTS .....	
WITH GATE SIMULATION .....	33
4.2.1. Intrinsic Spatial Resolution Experimental Measurement .....	
(NEMA phantom) .....	33
4.2.2. Intrinsic Spatial Resolution Simulation with GATE.....	34
4.2.3. Energy Resolution Test .....	37
4.2.4. Extrinsic Spatial Resolution Experimental Measurement .....	38
(with VXGP)	
4.2.5. Extrinsic Spatial Resolution Simulation Measurement(VXGP)...	39
4.2.6. Extrinsic Spatial Resolution - Experimental and Simulation .....	
Measurement (with LEGP) .....	40
4.2.7. Extrinsic Spatial Resolution Experimental and simulation .....	
Measurement with Scattering Medium (with LEGP).....	42
4.2.8. Extrinsic Spatial Resolution Experiment and Simulation .....	45
Measurement with Scattering Medium (with VXGP)	
4.2.9. Sensitivity Planar Measurement with (VXGP and LEGP) .....	46
5. RESULTS & DISCUSSION.....	50
6. CONCLUSION.....	53
7. REFERENCES.....	54
APPENDIX A : PRACTICE THE BUILDING GATE OF 8 STEPS .....	59
APPENDIX B : MY GAMMA CAMERA CODES FOR CYLINDRICAL PHANTOM .....	61
APPENDIX C : LINE SOURCE FOR VXGP COLLIMATOR.....	67
APPENDIX D : EXTRINSIC SPATIAL RESOLUTION SIMILATION DATA WITH VXGP FOR PHANTOMS.....	72
APPENDIX E : VXGP SCATTER EXTRINSIC TEST CODES.....	73
APPENDIX F : IMAGING OF PRO-ORGIN AND MATLAB .....	81

## LIST OF FIGURES

Figure 2.1.	Penetrating of radiation .....	5
Figure 2.2.	Imaging quality with high energy, low energy and low to medium energy .....	5
Figure 2.3.	The diagram illustrates the typical components found in a $^{99}\text{Mo} \rightarrow ^{99\text{m}}\text{Tc}$ radionuclide generator .....	6
Figure 2.4.	Simplified radioactive decay scheme for $^{99}\text{Mo}$ .....	9
Figure 2.5.	Components of a gamma camera .....	11
Figure 2.6.	Collimator, photomultiplier tubes and crystal Structure.....	12
Figure 2.7.	Detection by the NaI crystal and PM.....	13
Figure 2.8.	Optical to electrical signal conversion.....	14
Figure 2.9.	Photoelectric effect.....	20
Figure 2.10.	Compton scattering.....	21
Figure 3.1.	Gate simulation architecture.....	26
Figure 4.1.	VXGP Crystal geometry calculation .....	28
Figure 4.2.	Appearance of $45^\circ - 45^\circ$ angle.....	29
Figure 4.3.	Appearance of $0^\circ - 90^\circ$ angle .....	29
Figure 4.4.	Appearance of $-45^\circ - 45^\circ$ angle. ....	30
Figure 4.5.	Fwhm shape.....	32



Figure 4.6.	Lead marks used to measure the intrinsic spatial resolution in the y-direction...	33
Figure 4.7.	Placing of Nema phantom .....	34
Figure 4.8.	Intrinsic spatial resolution for GATE simulation .....	35
Figure 4.9.	Comparison of spatial resolution and FWHM for NEMA collimator ...	36
Figure 4.10.	Intrinsic resolution as a function of energy for GATE simulation .....	36
Figure 4.11.	WHM measurement for NEMA phantom for GATE simulation with proOrigin program (count-distance) .....	37
Figure 4.12.	Placement of the line sources for the Extrinsic spatial resolution VXGP .....	38
Figure 4.13.	Two line Tc-99m source for gamma camera.....	39
Figure 4.14.	GATE simulation for extrinsic spatial resolution test (VXGP).....	39
Figure 4.15.	Comparison of spatial resolution and FWHM for VXGP collimator.....	41
Figure 4.16.	Comparison of spatial resolution and FWHM for LEGP collimator .....	42
Figure 4.17.	Extrinsic test for scattering medium with LEGP collimator .....	43
Figure 4.18.	With Scattering medium for two line source for gamma camera.....	43
Figure 4.19.	Gate simulation for scattering medium for two line source .....	43
Figure 4.20.	Comparison of spatial resolution scatter and FWHM for LEGP collimator .....	44
Figure 4.21.	Comparison of spatial resolution scatter and FWHM for VXGP collimator .....	45

Figure 4.22.	Sensitivity test for distance 10 <i>cm</i> .....	46
Figure 4.23.	Sensitivity test for distance 40 <i>cm</i> .....	47
Figure 4.24.	Energy spectrum of sensitivity test.....	47

## LIST OF TABLE

Table 2.1.	Examples of the most popular Radioisotopes used in clinical studies .....	8
Table 2.2.	Radionuclides frequently used in medical imaging.....	9
Table 4.1.	System specification of VXGP(Vertex General Purpose ) collimator .....	28
Table 4.2.	System specification dedector type .....	28
Table 4.3.	Scatter percentage for NaI crystal <i>cm</i> .....	30
Table 4.4.	Scatter percentage for YAP crystal <i>cm</i> .....	31
Table 4.5.	Scatter percentage for YAP crystal <i>cm</i> .....	31
Table 4.6.	Scatter percentage with 7 different crystal (2.000.000 ) .....	31
Table 4.7.	Intrinsic Spatial Resolution (NEMA phantom ).....	35
Table 4.8.	Extrinsic spatial resolution- VXGP test results.....	39
Table 4.9.	LEGP specifications.....	41
Table 4.10.	Extrinsic spatial resolution with LEGP .....	41
Table 4.11.	Extrinsic spatial resolution scatter LEGP collimator .....	44
Table 4.12.	Extrinsic spatial resolution scatter VXGP collimator .....	46
Table 4.13	Measurment for sensitivty planar testing (VXGP and LEGP. ....	49

## LIST OF ABBREVIATIONS

	Energy
$R_i$	Decay corrected count rate
$T_{acq,i}$	Duration of the $i$ 'th acquisition
$T_{cal}$	Time of the activity calibration
$T_{half}$	Half life of radionuclide
$\alpha$	Alpha
$\beta$	Beta
	Gamma
	Lambda
BGO	Bismuth Germinate oxide
<i>Bq</i>	Becquerel
CERN	The European Organization for Nuclear Research
Ci	Curie
CT	Computerized Tomography
DTPA	Diethylenetriaminepenta-acetic
FOV	Field of view
FWHM	Full width at half maximum
Hex	Hexagon
LEGP	Low Energy General Purpose
LSO	Lutetium Orthosilicate
MC	Monte Carlo
MRI	Magnetic resonance imaging
NEMA	National Electrical Manufacturers Association
PET	Positron emission tomography
PM	Photomultiplier Tube
PMT	Photomultiplier tube
RF	Radio frequency

SPECT	Single photon emission computerized tomography
VXGP	Vertex General Purpose

## 1. INTRODUCTION

Monte Carlo simulations are useful for optimizing and assessing Gamma Camera, Single Photon Emission Computerized and Positron Emission Tomography protocols, especially when aiming at measuring quantitative parameters from Gamma Camera, SPECT and PET images [1]. Monte Carlo codes have been developed for Positron Emission Tomography (PET), Single Photon Emission Computerized Tomography (SPECT) and Gamma Camera GATE is a Monte Carlo simulation platform developed by the OpenGATE collaboration [2]. GATE simulation is an essential tool that can assist the design of new medical imaging devices. The simulation model is included Monte Carlo modelling of the camera collimator and back-compartment accounting for photomultiplier tubes and associated electronics. GATE [3] enables accurate simulation of Gamma Camera acquisitions. The subject of this dissertation is situated in the world of Monte Carlo Simulations of the Gamma Camera with GATE. Gamma Camera is used for in vivo volumetric imaging of 3-D distributions of radiopharmaceuticals. This imaging modality analysis radionuclides which emit single or multiple gamma rays during the radioactivity distribution in living tissues. The distribution of gamma photons is detected at various positions by using one rotating gamma camera. There are several studies made with GATE and Gamma Camera.

Uwe Pietrzyk et al, (2012), in their work, they have introduced Gamma camera in EduGATE. Various coordinates of the detected gammas, which corresponds to the location of the detection of the gammas in the crystal and difference material were selected for collimator at simulation. Tc was used as the source.

K Assie et al, (2005), in their work, they had 5 different phantom for simulation and they obtained full width at half maximum. Using Indium- 111 source for SPECT enables modelling of energy spectra, spatial resolution, sensitivity with GATE.

Mehdi Momenzad et al, (2011) , in their work, they use different back-compartment, crystal and be useful for quantitative analysis of images and dosimetry at gamma camera.

Jochen Hammes et al., (2011), in their work, they modelled a planar image with gamma camera. They used geometric phantom (for thyroid nodules) for simulation with GATE. They obtained a realistic simulation of the Iodine-131. Scintigraphy of solitary hyperfunctioning thyroid nodules were possible with GATE.

Steven Staelens, (2003), in their work, they used low energy high resolution (LEHR) and medium energy general purpose (MEGP) collimators. They obtained the spectral distributions, energy resolution, sensitivity, scatter component and spatial resolution analysis of Gamma Camera with GATE.

Nico Lanconelli, (2007), in his work, he showed the importance of Monte Carlo simulations in modeling detectors for Nuclear Medicine. They simulated a parallel flood irradiation of 140 keV photons and they obtained energy spectra, photon fluxes, uniformity of response and spatial resolution of the system.

Wael M.Elshemey, (2012), in his work, he illustrated the scattered radiation effects on the extrinsic sensitivity and counting efficiency of a gamma camera. An evaluation of the effect of scattered radiation on the extrinsic sensitivity and counting efficiency of a medical gamma camera was investigated with the aid of a circular source. Such a source incorporated into account the effect of scattered radiation practically encountered when a patient was imaged using a gamma camera.

Andrew Rova, (2008), in this work. He has developed an integrated software suite implementing NEMA tests for nuclear medicine scintillation cameras.

In this thesis, there three main parts; first is the simulation (with GATE) of the Gamma Camera used in Yeditepe University Hospital Nuclear Medicine Department, the second is the performance tests of Gamma Camera and the third is comparing the experimental and simulated results.

## 2. IMAGING IN MEDICINE

Imaging using radioisotopes dates back to about 1950 and became more widely used in the 1960's with the more general availability of radioactive isotopes, produced as by products of nuclear energy programs. The imaging procedure requires the injection or administration of a small volume of a soluble carrier substance, labelled by a radioactive isotope. The blood circulation distributes the injected solution throughout the body [4]. Ideally the carrier substance is designed to concentrate preferentially in a target organ or around a particular disease process. The radioactive tracer is ideally just an emitter of  $\gamma$  rays with energies in the range 60–510 keV. The emitted photons leave the body, to be collimated and counted using a large area electronic photon detector, sometimes called an Anger camera. The gamma image is a map of the distribution of radioactivity throughout the body, brought about by the interplay of a relatively uniform distribution due to the blood circulation and preferential concentration or depletion, due to local metabolic processes. Three types of imaging are used. Gamma Camera, SPECT and PET. The simplest is a single projection or planar image, generically similar to a single projection  $\gamma$ -ray radiograph. Starting in about 1975, two tomographic techniques have been brought into clinical use, which can provide reconstructed 2-D gamma images. These are called SPECT, single photon emission computed tomography, and PET, positron emission tomography. PET is probably the most successful in terms of spatial resolution but by no means the most widely used clinical gamma tomographic technique [1].

Gamma imaging, as shall describe below. It is important to understand that relatively poor spatial resolution and signal to noise ratio are inherent problems for all gamma imaging methods in comparison with  $\gamma$ -ray or MR methods. There are two main reasons for this. First, the small concentrations of radioactive substance that can safely and ethically be administered, produce a relatively small gamma photon flux and thus the techniques are nearly always limited by statistical fluctuations in the numbers of counted photons. In other words, quantum mottle is a serious problem in most gamma images. Secondly, on their trip out of the body, gamma photons are subject to absorption and scattering by the same mechanisms that scatter X-rays. These interactions produce significant distortions of the



gamma image, especially at low gamma energies[2- 4]. The utility of gamma scanning lies not in very high spatial resolution but rather in its ability to monitor and image metabolic processes with very high sensitivity. Thus gamma imaging is almost exclusively used to produce functional images. Many atoms and molecules involved in specific metabolic functions, in both disease and health, can be tagged by a radionuclide. The earliest example is that of thyroid imaging. The thyroid gland naturally concentrates about % 90 of the body's iodine during normal metabolic function. Gamma imaging of the thyroid gland, using radioactive iodine to investigate metabolic disorders or possible tumours, exploits this natural iodine metabolism. Today, gamma imaging is used extensively in the diagnosis of most cancers throughout the body, of heart function and disease and some brain disorders [5]. Over the past thirty years there has been a steady development in radiopharmaceuticals, allowing a very wide range of disease processes to be investigated using one of the gamma imaging methods [6]. In recent years PET has established itself, first as a research tool and now as a clinical tool, in the investigation of both normal and pathological brain function through the measurement of cerebral blood flow and the metabolic uptake of fluorinated glucose. Just like -ray CT, the long-term future of gamma imaging in some applications is uncertain [7]. For the present, however, gamma imaging performs a unique role in medical imaging which no other technique can fulfill [6, 7].

## **2.1. GENERAL IMAGING CONSIDERATIONS**

For the best quality of the nuclear images, two conditions are essential: the body must absorb very little radiation and the detector must absorb as much radiation as possible.

Radiation that is absorbed by the body cannot reach the detector to form an image. Radiation that passes through the detector without being absorbed also cannot contribute to producing the image [8]. Familiarity with the principles of absorption is critical to understanding the design and operation of the gamma camera. When the absorption mechanisms are used to the best advantage, the best possible images will be produced. (shown in Figure 2.1). Penetrating radiation, such as X-rays and gamma rays, is necessary for imaging. The energy of this radiation determines its usefulness for imaging purposes. [9]. Because very low energy photons are absorbed in body tissues, they cannot be used for efficient image production. Although high energy photons emerge from the body, very few are absorbed in the detector, and they are not useful for producing images. Photons of low

to medium energy exist the body in sufficient numbers and are absorbed by the detector with satisfactory efficiency to be useful for nuclear imaging. Relatively little absorption in body, good detection efficiency and useful are illustrated in Figure 2.2 [8, 10].

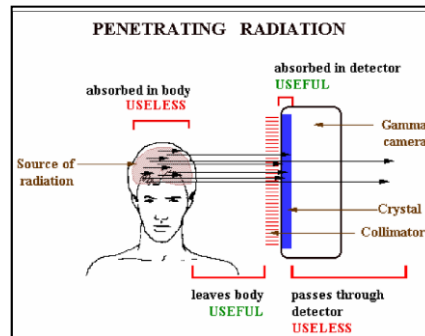


Figure 2.1. Penetrating of radiation [9]

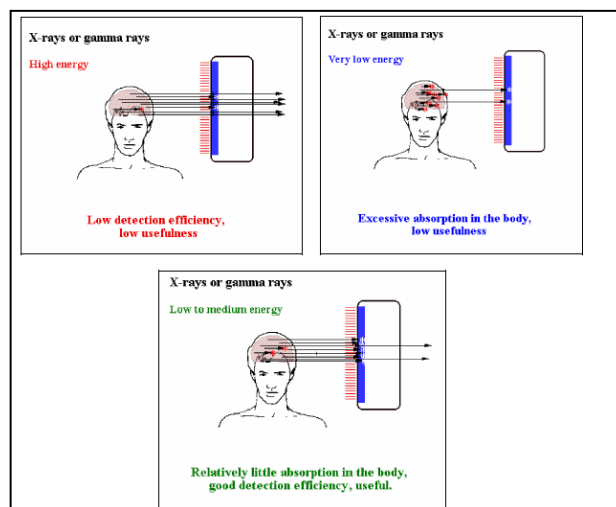


Figure 2.2. Imaging quality with high energy, low energy and low to medium energy [9]

## 2.2. RADIOPHARMACEUTICALS

### 2.2.1. The ideal Properties of Radionuclides and Carrier Molecules

In nature there are nearly 300 nuclei, consisting of different elements and their isotopes. Isotopes are nuclei having the same number of protons but different number of neutrons. They are elements having the same atomic number but different mass numbers. The

unstable nuclei decay by emission of  $\alpha$  or  $\beta$  particles or  $\gamma$  radiation. Some very heavy nuclei decay also by fission. Most of the radionuclides found in nature are members of four radioactive series (Thorium, Neptunium, Uranium, Actinium). Radioisotopes, because of their radiation characteristics and the energy they possess, can be utilized in industry, agriculture, healthcare and research applications. Nuclear reactions leading to radioisotope production are Radiative capture that This is primarily a thermal neutron reaction,  $(n, \gamma)$   $\beta^-$  decay,  $(n, p)$  reaction, Multistage reactions, Fission reaction, Cyclotron Produced Isotopes [10]. In nuclear medicine, the nuclide technetium-  $^{99m}\text{Tc}$ , is often mentioned in connection with *in-vivo* gamma irradiation. The parent nuclide of  $^{99m}\text{Tc}$  is  $^{99}\text{Mo}$  which is produced from the thermal fission of  $^{235}\text{U}$ . The fission yield of  $^{99}\text{Mo}$  is around 6%. The diagram illustrates the typical components found in a  $^{99}\text{Mo} \rightarrow ^{99m}\text{Tc}$  radionuclide generator as seen Figure 2.3. The design of the individual components will vary by manufacturer but will always allow for the separation and elution of the daughter radionuclide  $^{99m}\text{Tc}$  from the parent radionuclide  $^{99}\text{Mo}$  [12, 13]. The elution will result in a product that is sterile and free of impurities thus making it immediately suitable for human injection. The components in the typical generator are:

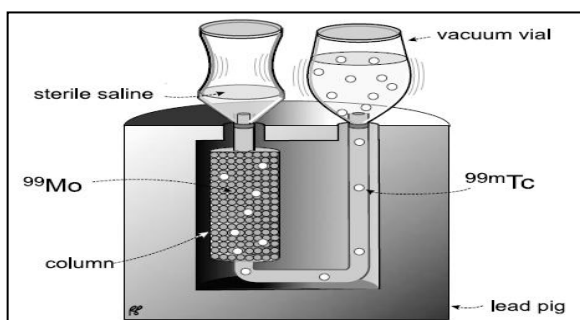


Figure 2.3. The diagram illustrates the typical components found in a  $^{99}\text{Mo} \rightarrow ^{99m}\text{Tc}$  radionuclide generator [13]

The column, usually glass, containing a bed of aluminium oxide as a support for the parent radionuclide.  $^{99}\text{Mo}$  (molybdate) will bind strongly to this support media and is not washed off during the subsequent elution of the daughter radionuclide  $^{99m}\text{Tc}$  (pertechnetate). A system of tubing that will allow the column to be washed with a sterile saline solution. The tubing will be medically approved since the liquids that contact this material may be injected into humans. The inlet tube will generally be accessible to the person who will be

collecting the  $^{99m}\text{Tc}$  from the generator, usually via a needle onto which a vial of saline can be attached as needed. Other designs provide an internal reservoir of saline for this purpose. The outlet tube is also accessible and generally terminates as a needle onto which an empty vial can be attached. Most generators use an evacuated vial for collection so that saline from the inlet side is drawn through the column and into the outlet vial. Filters will be found in generators in the form of porous frits, which serve to contain the alumina within the column, and usually a  $0.22\ \mu\text{m}$  filter which serves to remove any small particles from the eluted sample and to act as a safety device to ensure a sterile product. Lead shielding is required for operator safety. Both the parent and the daughter radionuclides emit radiation that must be absorbed. The glass column acts as a partial shield but can not stop the penetrating gamma radiation. All generators will provide a lead shield around the column and outlet tubing. Additional shielding is used during the collection process and of course the eluted  $^{99m}\text{Tc}$  must be shielded once it is collected from the generator. Generators are contained in a plastic housing and have some method (handles, straps) to allow manual or mechanical lifting and positioning. A generator with its lead shielding will weigh more than  $10\ \text{kg}$  depending on the manufacturer's design. There is a cover to protect the inlet and outlet needles and appropriate labelling on their generator housing. [11]. The generator described above is the one in general use and available from commercial suppliers. There have been various attempts to design other systems to produce  $^{99m}\text{Tc}$  generators but technical and product issues have prevented their widespread application. There are several ways of preparing the radiopharmaceutical with using the sign protein composite for example; DTPA (diethylenetriaminepenta-acetic ), Indium-111, Iodine-123, Technetium-99m. Radionuclide is connected to the component covalently. I use the radiopharmaceutical  $^{99m}\text{Tc}$ , Eczacıbaşı- MONROL manufacturing. It is transported as sterile in lead containers. Gamma imaging depends critically on the design and manufacture of suitable radiopharmaceuticals, substances that can take part in metabolism and are labelled with one or more gamma radioactive elements [5]. Apart from the ability to target a specific organ or disease, the substances must satisfy a number of criteria in order to be successful. Although a few radionuclides such as  $^{133}\text{Xe}$  and  $^{123}\text{I}$  are used in elemental form, the majority of radiopharmaceuticals consist of two parts: a carrier molecule and a suitable incorporated radionuclide. The choice of each part has its own constraints, the combination of the parts also needs careful consideration. Examples of the

Most Popular Radioisotopes Used in Clinical SPECT Studies are illustrated in Table 2.1 [12].

Table 2.1. Examples of the most popular Radioisotopes used in clinical SPECT studies [11]

Isotope	Half-Hife	Energy	Photon Abundance	Example of Clinical Application
<sup>99m</sup>	6	140	89	Brain, Heart, Cancer imaging, Thyroid (MIDI, HMPAO,DTPA)
<sup>67</sup>	3.26	93-185-300	38-21-17	Abdominal infection,Lymphoma, Cancer imaging(FREE)
<sup>111</sup>	2.80	171-245	21-17	Infections, Cancer imaging
<sup>123</sup>	13.2	159	83	Thyroid, Brain, Heart metabolism, Kidney(FREE, DTPA)
<sup>131</sup>	8.02	364	81	Thyroid cancer imaging, Metastasis detection ,Brain myocardial perfusion
<sup>201</sup>	3.04	167	11	myocardial perfusion
<sup>133</sup>	5.24	81	37	Lung ventilation , Brain imaging, Cerabral blood flow(DTPA)

In general, extremely small quantities of the labelled substance are actually administered to the patient, nevertheless great care has to be taken to ensure that the substance is not toxic and does not itself, unintentionally, alter the processes that are being studied. The carrier has to be soluble and eventually cross cell membranes, after oxidation or other metabolic processes [6, 13]. On the other hand, the carrier must be sufficiently stable that it has time to reach a target site and be concentrated there, before its metabolic demise. There are gamma-emitting radionuclides of biologically important elements such as iodine, fluorine and oxygen which allow a labelled, naturally occurring, biologically important molecule to be synthesised. More often, however, either a suitable radionuclide cannot be made or is too expensive to purify, then a compromise is sought in which a practical radionuclide, which has good properties for imaging, is chemically bonded to a synthesised carrier molecule which mimics the properties of a naturally occurring substance [5, 13].

### 2.2.2. Technetium

By far the most widely-used isotope in gamma imaging is <sup>99m</sup>Tc. In the hospital, a chemical generator, containing the high activity but longer lasting (longer half-life) precursor, <sup>99</sup>Mo, is used to separate the Tc atoms that are constantly being formed by radioactive decay of the parent <sup>99</sup>Mo. In Figure 2.4 , Simplified radioactive decay sheme for <sup>99</sup>Mo [12]. The Tc

is extracted when required in the form of sodium pertechnetate ( $Na+TcO_4$ ). This compound is then manipulated chemically to form a wide variety of different labelled carrier substances for different investigations [13]. Often the  $Tc$  atom is incorporated into a chelate structure, that is to say, into a chemical ring structure, in order to maintain the right degree of chemical stability within the body [14].

The  $\gamma$ -ray energy emitted by  $^{99m}Tc$  is 140 keV. This is ideal for gamma imaging. It is sufficiently high that photoelectric absorption within the body is quite small, but low enough for lead (again via the photoelectric effect) to be an efficient shield and collimator material. The half-life is just six hours, an extremely good match to natural clearance times in many metabolic processes [5, 15]. Radionuclides frequently used in medical imaging are illustrated in Table 2.2.

Table 2.2. Radionuclides frequently used in medical imaging [15]

Nuclide	Half Life (h)	Photon Energy (keV)	Method of Production
Molybdenum $^{99}Mo$	66	740	Fission
Technetium $^{99m}Tc$	6	140	Chemical generator

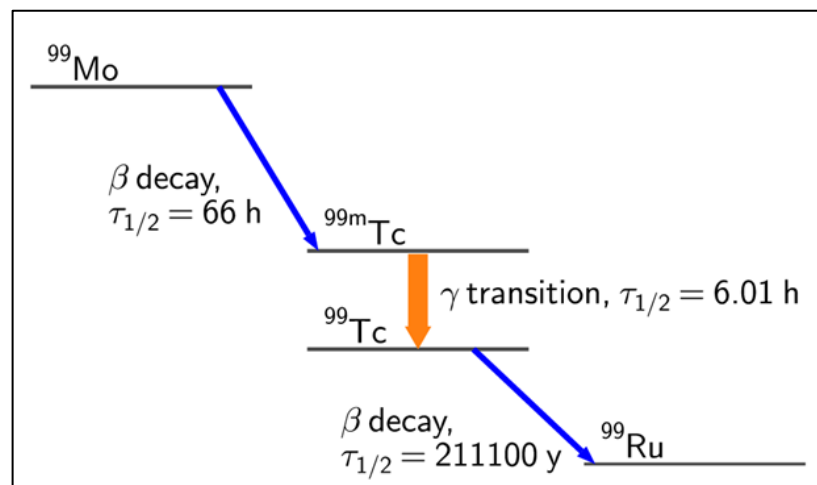


Figure 2.4. Simplified radioactive decay scheme for  $^{99}Mo$  [15]

### 2.3. GAMMA CAMERA COMPONENTS

All modern applications of gamma imaging use one or more large area multi-detectors, called gamma or Anger cameras, named after the inventor [12]. A standard arrangement is shown in Figure (2.5). The gamma camera is used in both planar imaging and SPECT studies [5].

The gamma camera includes the following components:

- The collimator, which focuses the gamma sources onto the *NaI* (Sodium Iodide) crystal.
- The crystal, which detects incoming gamma rays.
- Photomultiplier (PM) tubes and preamplifiers, which convert the light produced by the interaction of the gamma ray and the crystal into an electronic signal.
- Amplifiers and summation circuits, which combine individual signals and allow calibration of the gamma camera output.
- A discriminator, which ensures that only detected gammas with the appropriate energies are displayed. The discriminator emits a Z- pulse, which carries that information to the display.
- X and Y positioning circuits, which examine signals from individual PM assemblies and determine the position of the gamma on the crystal. This position information is carried to the display via + X, -X, +Y, and -Y signals.
- A visual display with display electronics, which depicts the corresponding position of the gamma on a screen. Components of a Gamma Camera as seen in Figure 2.5.

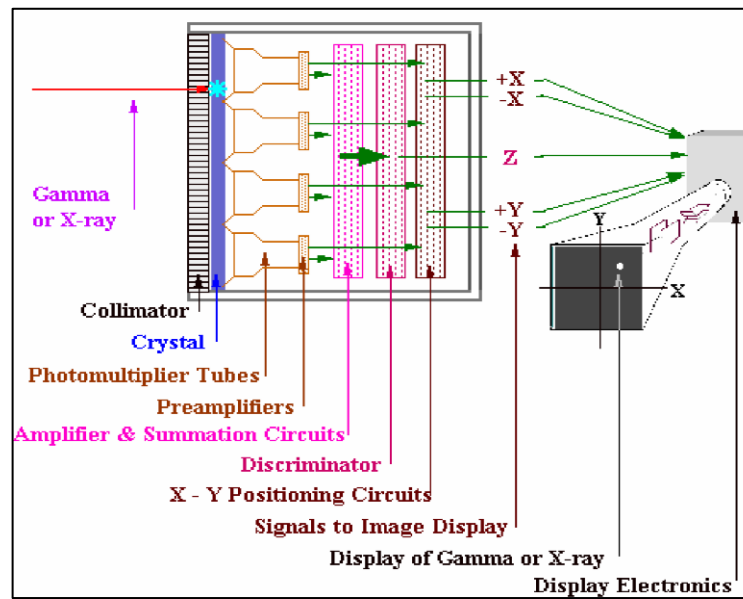


Figure 2.5. Components of a gamma camera [14]

### 2.3.1. Collimator

The collimator absorbs all the radiation that reaches the crystal except that which is located directly opposite the position of the tumor. In this way, a one-to-one relationship is established between the biodistribution of the radiopharmaceutical and the detecting crystal surface [9, 14-16].

- In a nuclear imaging study, a radiopharmaceutical is injected into a patient and is taken up by a tumor.
- Penetrating radiation is then emitted from the tumor in all directions.

If the gamma camera is used without a collimator, the radiation coming from the tumor will strike the surface of the entire camera crystal. In this situation, the crystal would be flooded with radiation, and the camera image would not show the tumor [12].

Adding a collimator makes a big difference [9, 12-16]. The tumor is now clearly visible on the camera image. As seen in Figure 2.6 .



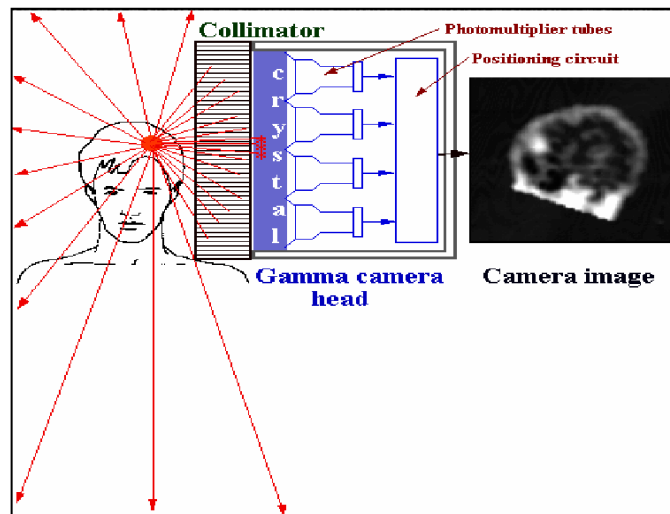


Figure 2.6. Collimator, photomultiplier tubes and crystal Structure [14]

### 2.3.2. Types of Collimators

A gamma camera is usually equipped with several interchangeable collimators. There are four types of collimators:

- The parallel-hole collimator
- The converging collimator
- The diverging collimator
- The pin-hole collimator

The parallel-hole collimator forms an image that is the same size as the source. The converging collimator forms a magnified image of the source. The diverging collimator, usually a converging collimator inserted backward, forms an image that is smaller than the source [9]. The pin-hole collimator forms a greatly magnified image. Collimator parameters such as the number and size of the collimator holes and the thickness of the septa also vary. Differences in these parameters affect the camera's field of view, image magnification ability, resolution and sensitivity [16]. The operator must be aware of these differences and their effect on the camera image in order to select the best collimator for a particular application.

### 2.3.3. Detection by the *NaI* Crystal

The Photomultiplier Tube (from now on PM) is the first component necessary for measuring the energy of individual incoming gammas. At diagnostic nuclear energies, the gamma or *X*-ray usually deposits all its energy in the Sodium Iodide (*NaI*) crystal via photoelectric interaction. The energy transferred to the crystal produces excitations that cause the emission of many lower energy light photons. The number of light photons released is proportional to the energy of the incident gamma or *X*-ray. As seen in Figure 2.7 [9, 17].

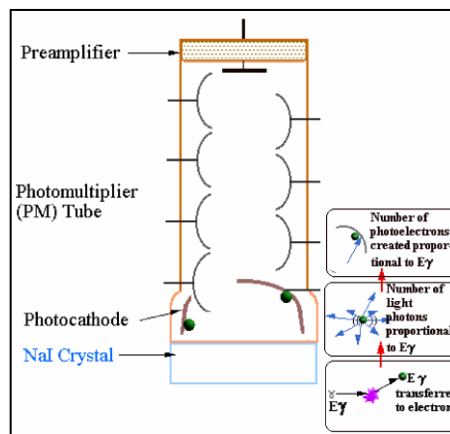


Figure 2.7. Detection by the *NaI* crystal and photomultiplier tube [14]

### 2.3.4. Optical to Electrical Signal Conversion

The PM tube is the first component necessary for measuring the energy of individual incoming gammas [9]. The gamma or *X*-ray usually deposits all its energy in the Sodium Iodide (*NaI*) crystal via photoelectric interaction. The energy transferred to the crystal produces excitations that cause the emission of many lower energy light photons. The number of light photons released is proportional to the energy of the incident gamma or *X*-ray [17]. (As seen in Figure 2.8.)

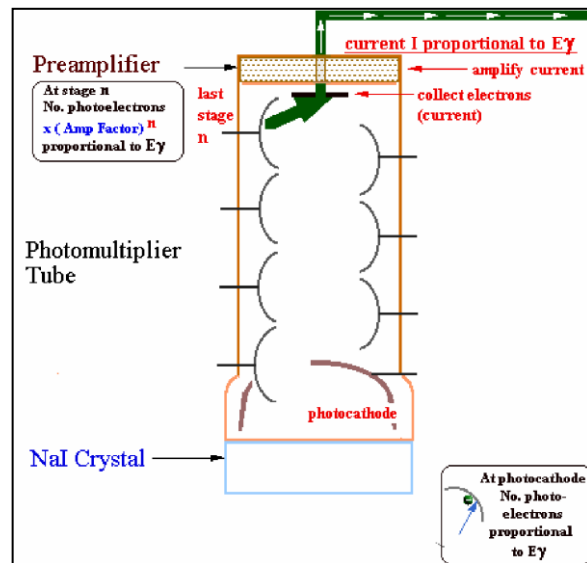


Figure 2.8. Optical to electrical signal conversion [14]

### 2.3.5. PM Tube Signal Amplification

The photomultiplier tube has several stages, the first of which is the photocathode. Each stage is at a positive voltage relative to the stage before it. Electrons are ejected from one stage surface and are accelerated to the next higher stage [8]. The energy each electron gathers during acceleration allows it to knock out additional electrons from the next surface. This produces an electron amplification factor for each stage. At each stage, the electron multiplication process is repeated. [14]. Therefore, the total signal at each stage is calculated as the original electron signal multiplied by the amplification factor as many times as there are stages. The primary number of photoelectrons times the amplification factor for each stage is proportional to the energy of the gamma. Because so many electrons are involved, the output of the PM tube is characterized as a current pulse,  $I$ , rather than as individual electrons [2, 18]. The current pulse is a measure of the energy of the original gamma or X-ray. The Gamma Camera uses a large number of PM tubes, each placed on a large crystal. Each performs measurements that are specific to its location on the crystal.

### **2.3.6. Electronic Amplification**

The magnitude of the current-pulse emerging from the PM tubes and the preamplifier can be adjusted with an electronic amplifier. The measure of the output of the amplifier is given as the maximum voltage or peak of the pulse [5]. This peak voltage is therefore a measure of the original incidence gamma or X-ray energy. For example, the amplifier can be adjusted so that a detected 140 *keV* gamma results in a pulse of 1.4 *volts* [9]. Other detected gamma energies will result in corresponding voltage pulses.

### **2.3.7. Signal Energy Calibration**

Gammas with known energies are used to energy calibrate the gamma detection system. The amplifier is adjusted so that detected energies have a voltage signal value that is standard for that particular energy (For example, 1.40 *volts* for 140 *keV*). If the height of the voltage pulse is too high or too low, the amplifier is adjusted to standardize the height of the pulse [5, 9]. This process determines the energy scale. Any other energies detected will be proportional to this calibration energy (For example, 3.61 *volts* for 361 *keV*).

### **2.3.8. Energy Discrimination**

Although photons have the same energy, they do not all produce the same energy measurement. As shown previously, the photopeak detected from a given gamma energy is spread over a range of energies centered on the peak energy. Therefore, an electronic window can be set with maximum and minimum energies. Each detected photon can be stored as to whether it is within or outside the window [9].

### **2.3.9. Energy Measurement**

When a gamma ray is absorbed by the crystal, the crystal releases a flash of light photons that emanate in all directions. The PM tubes closest to this event intercept most of these photons [9]. Because the PM tubes are distributed evenly over the crystal's surface, the signal generated by summing the output of all the photomultiplier tubes is independent of the gamma's position on the crystal. The exception to this rule occurs at the edge of the

crystal, where light reflections increase signal size or create edge effects. These are examples of flood images in which the crystal is uniformly irradiated. They demonstrate the phenomenon known as edge packing [18]. A gamma camera will cut off the image at a dimension smaller than the crystal to eliminate the appearance of edge packing [9]. Once through the collimator, the incident  $\gamma$ -rays produce low energy scintillation photons in the thallium-activated sodium iodide,  $NaI(Tl)$ , crystal and these are detected by the PM tubes. In modern, multi-purpose systems, two large area cameras are used simultaneously in order to intercept more of the emitted  $\gamma$ -rays [17]. Each gamma camera has one, large area single crystal of  $NaI(Tl)$  backed by many PM tubes [19]. There are two square gamma cameras which can be rotated independently around the patient to produce SPECT data, or held fixed to produce a planar scan [16]. A single crystal of  $NaI(Tl)$  is essential to ensure that the secondary photon light can travel, without attenuation, throughout the scintillator volume and enter as many of the PM tubes as possible. A fraction of the total scintillation light produced by each gamma event enters the PM tubes [9, 19-20].

### **2.3.10. Gamma Camera Performance**

The spatial resolution and sensitivity of the gamma camera are determined by the geometry of the collimator, gamma photon scatter and absorption, both within the patient and within the collimator, and finally, the statistical uncertainty associated with a relatively small number of counts per image pixel. The following sections describe the main factors determining performance [5, 21].

## 2.4. NUCLEAR MEDICINE IMAGING

Nuclear Medicine imaging is a non-invasive imaging technique which uses radioisotopes to image biological processes within the body. They are generally labelled with a compound which targets a particular area of pathologic interest. The radioisotope undergoes radioactive decay and emits gamma rays and/or subatomic particles. Gamma rays which exit the body are detected by an external radiation detector to produce an image. While the uptake of some radiotracers may show some anatomical information, it is predominantly used to highlight areas of pathology and biologic processes such as tissue perfusion and glucose metabolism [7].

There are two main types of nuclear medicine imaging, single photon emission computed tomography (SPECT) and positron emission tomography (PET). The fundamental difference between the two is the detection of one gamma ray versus two coincident gamma rays as needed to create an image [20]. SPECT, images are acquired from single gamma rays emitted from radiotracers which are incident on gamma cameras whereas PET uses a positron emitting radiotracer. The positron undergoes annihilation with an electron, emitting two 511 keV photons at 180°. Coincident detection (within a specified time window) of the annihilation photons results in a detected event. Planar images are two dimensional projections of the tracer distribution through the body. A cross sectional image of the body is composed of multiple planar images at varying angles called tomographs [6].

### 2.4.1. Multimodality Imaging

Multimodality imaging has become an indispensable tool in diagnosing diseases, aiding in treatments and surgeries. PET/CT (X-ray computed tomography) and SPECT/CT are the most common multimodality imaging systems and have been widely used for oncology applications. A multimodal system allows one to correlate functional information with anatomical references and it allows for better image registration due to a common patient support, thus making it more convenient and potentially more cost effective to perform image acquisition simultaneously or sequentially. While there are many advantages to this technology and the modalities of imaging used, there are some drawbacks to the ones in

current clinical use. Patients are exposed to a larger amount of radiation as a result from  $\gamma$ -rays and the injected radiotracers. Magnetic resonance imaging (MRI) is an alternative imaging modality to CT which requires no ionizing radiation. Nuclei in the body that have an odd number of protons possess an intrinsic angular momentum called spin. Hydrogen is the most abundantly used nuclei in MRI imaging, which consists of a single proton. Three major components of MRI hardware include the main magnetic field (1.5-7T), a radio-frequency (RF) pulse and the magnetic field gradients. The main magnetic field is used to aligns the nuclei to an equilibrium state. The RF pulse is used to change the local magnetization of the nuclei during image acquisition and the magnetic field gradients are used to provide spatial localization [9]. Besides the benefit of no exposure to ionizing radiation, MR may be superior to other anatomical imaging techniques due to its ability to obtain somefunctional information and its excellent soft tissue contrast . There has been significant development in multimodality imaging in the past decade with PET and MR; however, little development of SPECT/MR has been done. Since SPECT imaging has many more applications than PET, it stands to reason that SPECT/MR could have a greater clinical impact. PET is widely used for oncology applications; however, SPECT can be used for cardiac, brain, renal and bone [4]. Depending on the type of imaging one of the fundamental challenges in incorporating these modalities is that the gamma camera is not operable in a magnetic field . Gamma cameras consist of a scintillator coupled to a photomultiplier tube (PMT) [20]. Inside the photomultiplier tube, electrons are accelerated across voltage potentials to generate a signal. In the presence of a magnetic field, the trajectory of the electron would be altered, thus distorting the signal [21]. As a result, there are researches undergoing about a new type of semiconductor detector andsilicon photomultipliers which have been reported to be insensitive to magnetic fields as an alternative to photomultiplier tubes [22]. Provided the magnetic field from MRI doesn't affect the performance of silicon photomultipliers and the accompanying electronics [4, 23].

## 2.5. RADIATION INTERACTIONS

The discussion of interactions of radiation with matter is important before delving into the physics of detecting radiation. Photon interaction with a material can occur in one of the several ways which include:

- The photoelectric effect
- Compton scattering
- Pair production

Depending on the energy of the photons, there is an associated probability that it will undergo a particular interaction represented by the cross section [5, 8, 24]. At lower energies and high  $Z$  (atomic number) materials, the probability of the photoelectric effect dominates, whereas Compton scattering will more likely occur at higher energies and lower  $Z$  materials [24]. Pair production will only occur if the photon energy exceeds 1.022 MeV (the sum of the rest mass of an electron and its antiparticle, the positron) [6]. In nuclear medicine we are generally interested in relatively lower energy photons, so pair production is not a significant interaction. However, it should be noted that some radio tracers in nuclear medicine do emit high energy gamma rays in which case, pair production would be relevant [6, 25]. The following is a brief description of the relevant interactions.

### 2.5.1. Photoelectric Effect

When a gamma ray of sufficient energy (greater than or equal to that of the binding energy of the electron) is absorbed by the atom, a bound electron is ejected from the atom [14]. The ejected electron has energy equal to the difference between the binding energy of the electron shell and the incident photon. Since photoelectric absorption increases with the strength of electron binding, photons are generally ejected from the K shell [6, 22, 25]. Photons with energy below the K shell binding energy will go on to interact with electrons in the L and M shell. Photoelectric Effect shows in Figure 2.9.



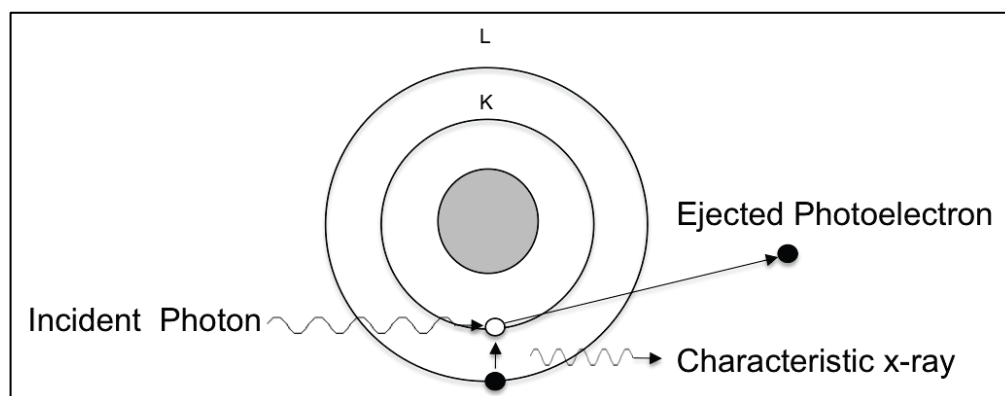


Figure 2.9. Photoelectric effect [6]

A vacancy exists from where the electron was ejected [17]. To stabilize the atom, an electron from an outer shell will fill the hole while emitting a characteristic X-ray with energy equal to the difference between the two energy levels. In low  $Z$  materials, the characteristic  $X$ -ray energy is on the order of a few keV, whereas in high  $Z$  material the energy could be on the order of 20-100 keV [20]. Therefore, for interactions occurring within the body, energy from these x-rays is generally negligible. For high  $Z$  materials, the  $X$ -rays may contribute to background [6, 7]. Additionally, the characteristic x ray may go on to eject an electron from an outer shell provided the energy is equal to the binding energy of the electron [11]. The release of this electron is known as an Auger electron and since the photon is absorbed in the Auger electron, radiation is not emitted. Therefore as the atomic number increases, the probability of the photoelectric effect interaction occurring increases significantly [6, 13, 17, 24-27].

### 2.5.2. Compton Scattering

Compton scattering is an inelastic scattering interaction which is highly probable when the incident photon energy is much larger than the binding energy of the innermost electron. Since the photon energy is much larger than the binding energy of the atom, it is approximated that the interaction occurs between the photon and a loosely bound or free electron. Due to the massless nature of the photon, to maintain energy and momentum conservation, the photon scatters and energy is transferred to the recoil electron. Compton Scattering shows in Figure 2.10 .

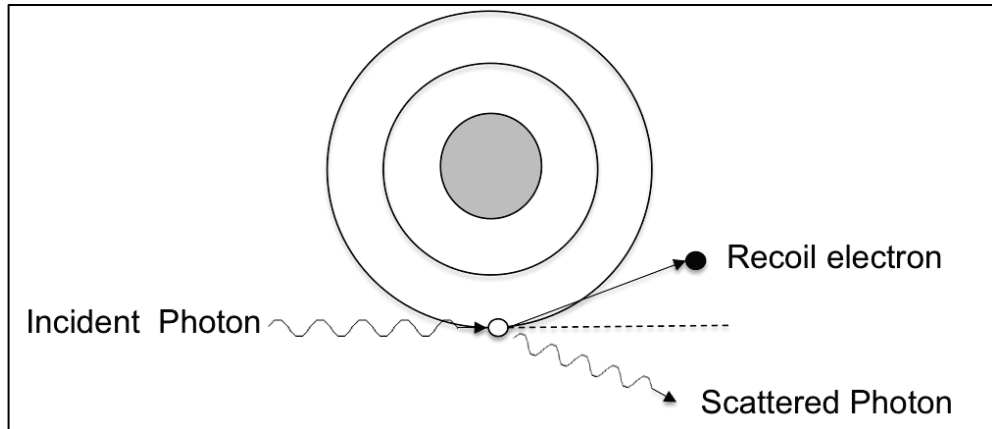


Figure 2.10. Compton scattering [6]

From energy and momentum conservation, the wavelength of the scattered photon  $\lambda$  is related to the wavelength of the incident photon  $\lambda_0$  where  $m_0$  is the rest mass of an electron and  $\theta$  is the angle between the incident and scattered photon [6, 7]. This equation can also be represented in terms of the energy of the photons by substituting .

$$\lambda - \lambda_0 = \frac{h}{m_0 c} (1 - \cos \theta) \tag{2.1}$$

$$\frac{1}{\lambda} - \frac{1}{\lambda_0} = \frac{m_0 c}{h} (1 - \cos \theta) \tag{2.2}$$

$$\frac{1}{\lambda} - \frac{1}{\lambda_0} = \frac{m_0 c}{h} (1 - \cos \theta) \tag{2.3}$$

According to equation (2.1- 2.3), if the angle is  $0^\circ$  the photon does not scatter because its scattering energy is equal to the initial energy and since there is no energy transfer, no scattering occurs [6, 7]. In Compton scattering, the photon scattering angle can only approach  $180^\circ$  in which the scattered photon energy approaches the initial photon energy which is the maximum scattered photon energy [22, 27]. The scattered photon may range from anywhere from  $0$  to  $\lambda_0$ . However, the angle at which the energy transfer to the recoil electron is a maximum (when the energy transferred to the scattered photon is a minimum) is at  $180^\circ$  as seen in equation (2.4) .

---

---

(2.4)

### 2.5.3. Pair Production

Occurs when a high energy gamma passes close to a nucleus [19]. Its energy is converted into a positron electron pair. For this conversion to occur, the gamma must have an energy of at least magnitude are not encountered in nuclear diagnostic imaging; therefore, pair production is of no consequence in nuclear imaging.

### 3. MONTE CARLO SIMULATIONS

Monte Carlo is a numerical calculation method based on random variable sampling. It is a statistical method that uses random numbers as the base to perform simulation of any specified situation. All Monte Carlo codes share some common components, such as random number generator, rules to sample probability distributions, and sets of probability density functions [3]. The features that make the codes different are related to the accuracy, flexibility, efficiency and ease to use of the codes. With the advent of personal computers and the popularization of faster computational machines, the Monte Carlo simulations have been increasing popular as an important alternative for the solution of complex problems. In most Monte Carlo applications, the physical process can be simulated directly. It only requires that the system and the physical processes can be modeled from known probability density functions [25]. There are several SPECT/PET dedicated Monte Carlo software packages developed for simulating a variety of emission tomography studies. Among them, public domain codes have been made available in last years, allowing the use of the Monte Carlo method by the whole scientific community and even in the clinical environment [26]. Two types of Monte Carlo codes can be used for simulating Gamma Camera, SPECT and PET:

- General purpose code, which simulate particle transport and were initially developed for high energy physics or for dosimetry.
- Dedicated codes, designed specifically for SPECT or PET simulations [27].

Monte Carlo simulations have been extensively used for the optimization of collimator design parameters such as hole size, septal thickness, collimator height and also collimator type can also be investigated [28]. Throughout this thesis, GATE application for Gamma Camera has been used as a Monte Carlo tool for the whole my Gamma Camera simulation. However, except for GATE, also needed to develop new fast and user friendly Monte Carlo tool, collimator efficiency and optimize collimator of my Gamma Camera within a short time.

### 3.1. GATE

GATE is an advanced opensource software developed by the international OpenGATE collaboration and dedicated to numerical simulations in medical imaging and radiotherapy. It currently supports simulations of Emission Tomography (Positron Emission Tomography - PET and Single Photon Emission Computed Tomography - SPECT), Computed Tomography (CT) and Radiotherapy experiments. Using an easy to learn macro mechanism to configurate simple or highly sophisticated experimental settings, GATE now plays a key role in the design of new medical imaging devices, in the optimization of acquisition protocols and in the development and assessment of image reconstruction algorithms and correction techniques. It can also be used for dose calculation in radiotherapy experiments. Gate is a program in which the user interface is based on scripts. Each command performs a particular function, and may require one or more parameters. The Gate commands are organized following a tree structure. For example, all geometry control commands start with geometry, and they will all be found under the */geometry/* branch of the tree structure. All functions in Gate can be accessed to using command lines. The geometry of the system, the description of the radioactive source(s), the physical interactions considered. Can be parameterized using command lines which are translated to the Gate kernel by the command interpreter. In this way, the simulation is defined one step at a time and the actual construction of the geometry and definition of the simulation can be seen on-line. If the effect is not as expected, the user can decide to re-adjust the desired parameter by re-entering the appropriate command online. Although entering commands step by step can be useful when the user is experimenting with the software or when he/she is not sure how to construct the geometry. Commands that led to a successful simulation. Macros are ASCII files (with '.mac' extension) in which each line contains a command or a comment [2]. Comments start with the character '#'. Macros can be executed from within the command interpreter in Gate [28]. A macro or set of macros must include all commands describing the different components of a simulation in the right order. Usually these components are visualization, definitions of volumes (geometry), systems, digitizer, physics, initialization, source, output and start. These steps are described in the next sections [29]. To execute a macro (mymacro.mac in this example) from the Linux prompt, just type: I use GATE: A Geant4, Version v6.2 application that developments CERN collaboration (> 10 years) In addition, distribution of GATE through

VIRTUAL MACHINES (Virtual Box) for user's convenience. Users write their own Geant4-based programs (C++). The system name of the Gamma Camera in GATE. I want to explain GATE World. The World is the only volume initially present in GATE. [28]

### 3.1.1. The building GATE of 8 steps

- The World is the only volume initially present in GATE. The World volume is essential.
- Building a geometry that A new volume must be the daughter of an another volume. (user's geometry set X-Y-Z Length, set Material solid type and dimensions).
- The material used must be in the Gate material database (GateMaterials.db) .Various material definitions (simple defined by number of atoms, fraction or can be edited to add new materials).
- Combining repeaters.
- Defined by Physics list -Using G4 models for physical processes (particle construction, Interactions for photons,electrons,positrons, radioactive decay).
- Initialisation.
- Building sources( model simple emission geometries).
- Run (ROOT analysis) (Figure 3.1) [12, 32].

Practice the building GATE of 8 steps were given in the APPENDIX A.

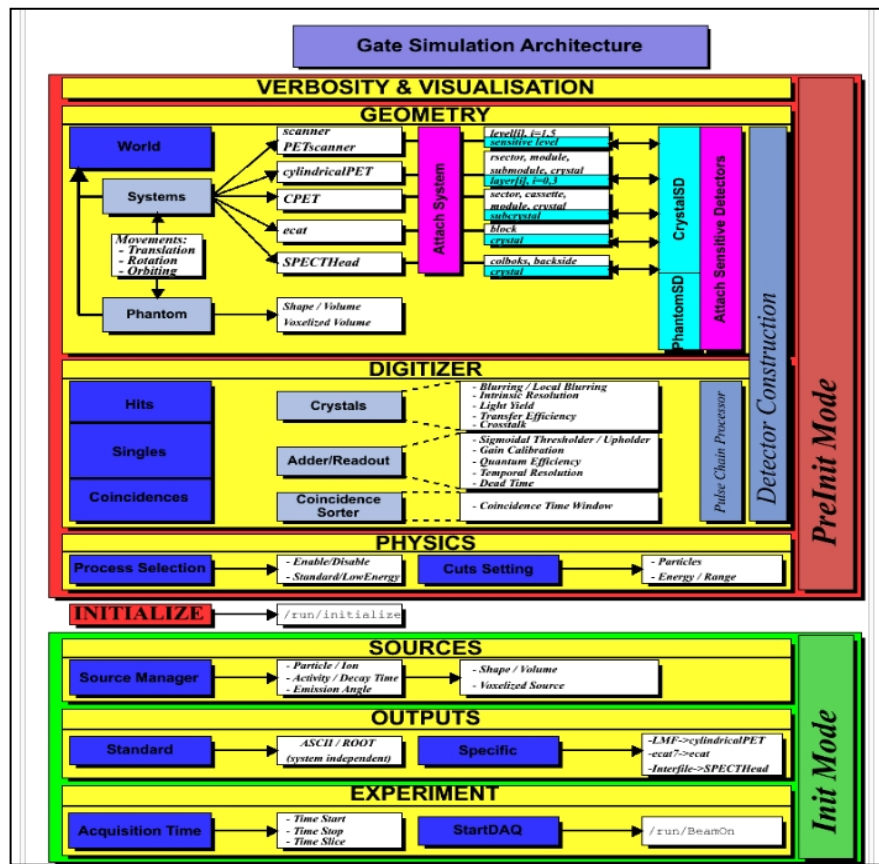


Figure 3.1. Gate simulation architecture [23]

### 3.2. ROOT OUTPUT FILE

Root cause analysis (RCA) is a method of problem solving that tries to identify the root causes of faults or problems that cause operating events. Very simple sinogram production during the simulation for many Gamma Camera, PET, SPECT, and This systems add new output channels. `gate/output/ROOT/` [1]

## 4. METHODS & MATERIALS

GATE is an advanced opensource software developed by the international OpenGATE collaboration and dedicated to numerical simulations in medical imaging and radiotherapy. It currently supports simulations of Positron Emission Tomography (PET) and Single Photon Emission Computed Tomography - SPECT), Computed Tomography (CT) and Radiotherapy experiments. Linux based GATE is used in this thesis.

Specification of PHILIPS-Forte Gamma Camera (used in Yeditepe University Nuclear Medicine Department) is chosen as the instrument to be simulated. Gamma Camera PHILIPS-Forte is also investigated experimentally with different phantoms according to NEMA procedures and the simulation is interpreted according to the experimental results to make sure that the specifications of the Gamma Camera modelled is the same with the one used in the Nuclear Medicine Department. The camera acceptance tests are all done according to NEMA procedures.

### 4.1. BASIC GAMMA CAMERA SIMULATION

Specifications of PHILIPS - Forte Gamma Camera are taken. The world in GATE is formed with the parts in the Gamma Camera such as the collimator, crystal and back-compartment. Afterwards, known collimator type, size, hole shape, septa, length and holes (see Table 4.1) are added to the GATE world as calculating the geometry for the system. In Figure 4.1, the hole geometry as hexagon can easily be seen. NaI crystal specifications are illustrated in Table 4.2. My Gamma camera codes for cylindrical phantom were given in the APPENDIX B.

In the Gamma Camera simulation, collimator is represented with the blue rectangle, NaI crystal with yellow rectangle and the back-compartment with gray rectangle (Figure 4.2). Green lines represented the gamma beam of  $^{99m}\text{Tc}$  source as the white dot in the yellow cylindrical shape phantom. ( Figure 4.3 - 4.4).



Table 4.1. System specification of VXGP (Vertex General Purpose ) collimator

Type	Hole Shape	Size	Septa	Length	Number of Holes
Vertex General Purpose (from now on VXGP)	Hexagon	1.78	0.152	42	58,700

Table 4.2. System specification dedector type

Non-anger digital dedector	Field of view (rectangular)	Crystal thickness	Imaging table type	Dimensions (cm)
1 ADC/ PMT	38.1 x 50.8 <sup>2</sup>	55 cm	High modulus carbon fiber	264 x66 cm <sup>2</sup>

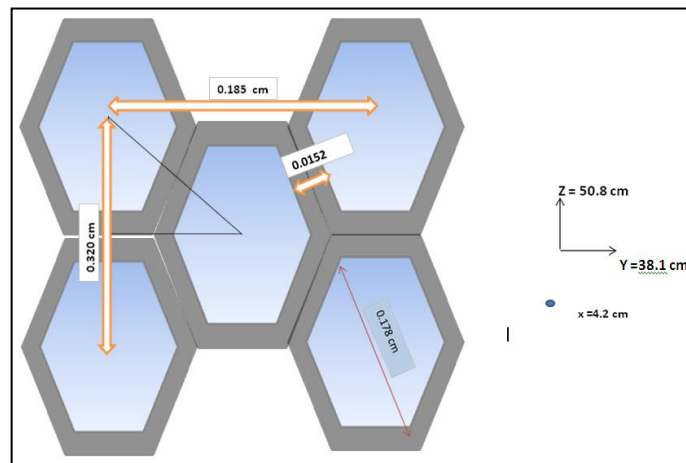


Figure 4.1. VXGP crystal geomety calculation

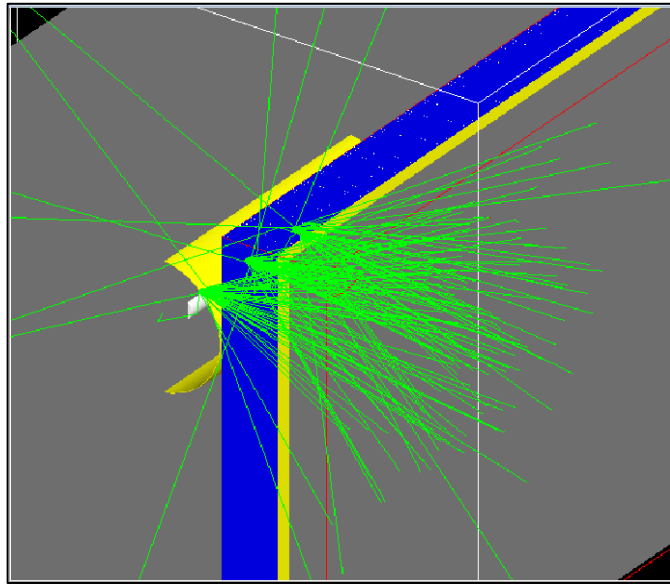


Figure 4.2. Appearance of 45 - 45 angle

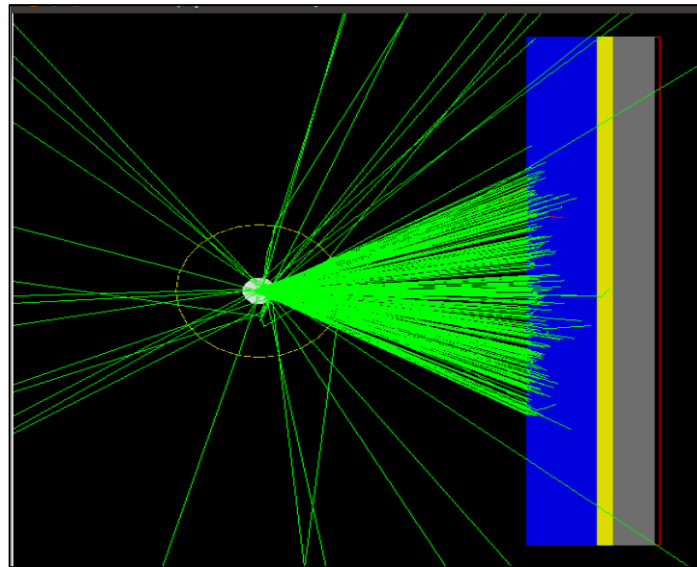


Figure 4.3. Apperance of 0 - 90 angle

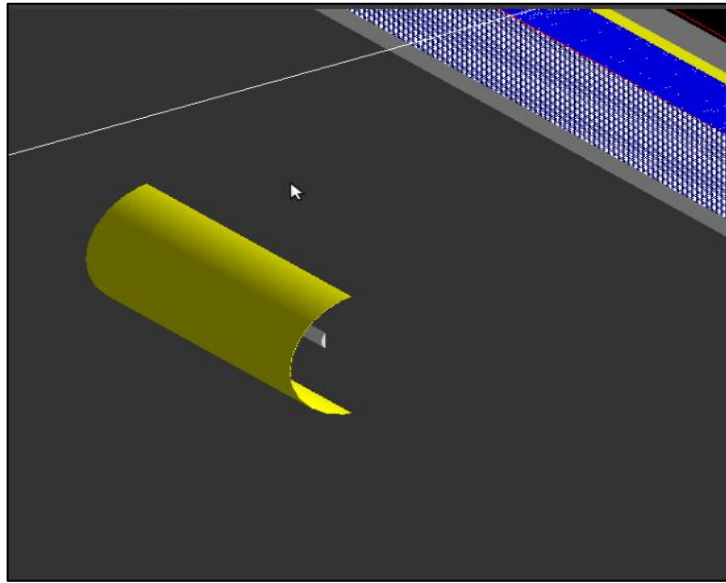


Figure 4.4. Appearance of  $-45^{\circ}$ - $45^{\circ}$  angle.

#### 4.1.1. Various Crystals with Different Thickness and Activities

After the geometry of PHILIPS-Forte Gamma Camera is done in GATE, the simulation is repeated with *NaI* crystal 2 cm in thickness with various activities as seen in Table 4.3, *YAP* crystal in 1 cm with various activities as seen in Table 4.4, *YAP* crystal in 2cm with various activities as seen in Table 4.5 and 7 different crystals (with 2.000.000 *Bq* activity) as seen in Table 4.6.

Table 4.3. Scatter percentage for *NaI* crystal 2 cm

Activity ( <i>Bq</i> )	Primary events (%)	Crystal scatt. (%)	Collimator (%)	Back- compartment (%)	Table (%)	Phantom(water) (%)
100	84.60	15.38	0	0	0	0
1000	77.63	14.47	1.31	1.97	0	4.60
10.000	79.47	14.70	0,26	2.20	0.06	3.27
100.000	79.57	14.40	0.50	2.28	0.04	3.14
2.000.000	80.01	13.30	0.66	2.87	0.06	3.07

Table 4.4. Scatter percentage for YAP crystal 1 cm

Activity <i>Bq</i>	Primary events (%)	Crystal scatt. (%)	Collimator (%)	Backcompartment (%)	Table (%)	Phantom(water) (%)
100	81.80	18.18	0	0	0	0
1000	53.19	34.04	0.70	7.09	0	4.96
10.000	49.60	37.50	0.47	9.15	0.07	3.02
100.000	50.56	35.60	0.48	10.06	0.01	3.14
2.000.000	50.54	35.96	0.55	9.83	0.03	2.99

Table 4.5. Scatter percentage for YAP crystal 2cm

Activity ( <i>Bq</i> )	Primary events (%)	Crystal scatt. (%)	Collimator (%)	Backcompartment (%)	Table (%)	Phantom(water) (%)
100	64.20	14.2	0	14.20	0	7.14
1000	49.18	34.4	0	13.11	0	3.27
10.000	52.56	36.5	0.46	7.95	0.07	3.43
100.000	48.91	39.7	1.23	8.00	0.034	2.93
2.000.000	50.7	36.6	0.55	8.80	0.03	3.04

Table 4.6. Scatter percentage with 7 different crystal (2.000.000 *Bq*)

	Primary events (%)	Crystal scatt. (%)	Collimator (%)	Backcompartment (%)	Table (%)	Phantom(water) (%)
NaI	79.60	14.50	0.46	2.13	0.02	3.15
LSO	88.00	8.26	0.45	0.01	0.02	3.18
BGO	90.21	6.11	0.44	0.03	0.02	3.19
YAP	51.00	36.00	0.53	8.70	0.03	3.06
GSO	85.00	11.00	0.46	0.04	0.02	3.24
CZT	80.00	15.00	0.48	0.57	0.02	3.17
PWO	90.80	5.44	0.44	0	0.02	3.27
LuAP	87.32	8.95	0.47	0.06	0.02	3.21

## 4.2. PERFORMANCE OF GAMMA CAMERA ACCEPTANCE TESTS WITH GATE SIMULATION

Quantification of nuclear medicine image data is a prerequisite for personalized absorbed dose calculations and quantitative biodistribution studies. The spatial response of a detector is a governing factor affecting the accuracy of image quantification, and the aim of this work is to model this impact. Monte Carlo (MC) simulations, using the codes GATE are used to investigate the extrinsic effect as a function of energy and its variation across the FOV (field of view). Gamma Camera's quality control tests are compared and should be convenient with the factory settings. These tests are called acceptance tests and should be done according to the NEMA (National Electrical Manufacturer's Association) procedures. In this thesis, most of the NEMA's acceptance tests are done such as system spatial resolution (extrinsic and intrinsic) for different collimators (VXGP and LEGP). These tests are *intrinsic spatial resolution test*, *energy resolution test*, *extrinsic spatial resolution test*(for VXGP collimator), *extrinsic spatial resolution test* (for LEGP collimator) and *extrinsic spatial resolution test with a scattering medium*. Full width at half maximum (from now on FWHM) is an expression of the extent of a function, given by the difference between the two extreme values of the independent variable at which the dependent variable is equal to half of its maximum value. (shown in Figure 4.5). Full width at tenth maximum (from now on FWTM) is an expression of the extent of a function, given by the difference between the two extreme values of the independent variable at which the dependent variable is equal to tenth of its maximum value. FWHM and FWTM results are calculated with the final version of MATLAB, ImageJ and OriginPro.

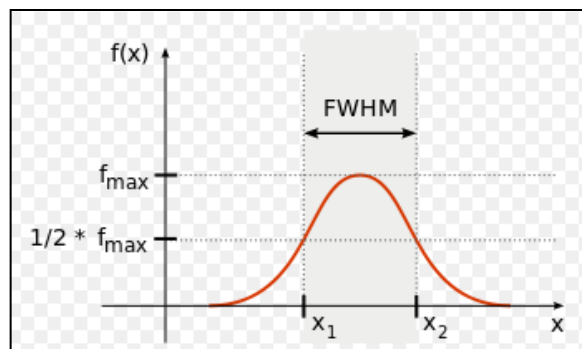


Figure 4.5. FWHM shape

#### 4.2.1. Intrinsic Spatial Resolution Experimental Measurement (NEMA phantom)

Spatial resolution refers to the size of the smallest object that can be resolved on the image. In a digital image, the resolution is limited by the pixel size, The smallest resolvable object cannot be smaller than the pixel size. The intrinsic resolution of an imaging system is determined primarily by the instantaneous field of view of the sensor, which is a measure of the ground area viewed by a single detector element in a given instant in time. This resolution can often be degraded by other factors which introduce blurring of the image. NEMA phantom is a planar phantom that has been designed with 3 lead band and 1 air space form. (shows Figure 4.6).

Construction of the test:

- Collimator is removed, dedector's surface is placed according to the source (as seen in Figure 4.7)
- NEMA phantom is placed on the detector.

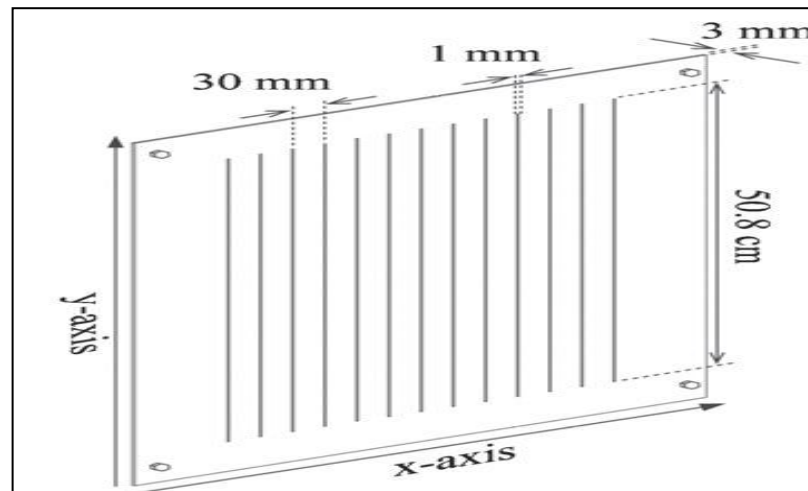


Figure 4.6. Lead marks used to measure the intrinsic spatial resolution in the y-direction

Preparation of the point source:

- Volume of less than  $1\text{ cm}^3$  of  $^{99\text{m}}\text{Tc}$  is placed over the center of the detector about 10 cm away.



Figure 4.7. Placing of NEMA phantom

- Properties of image taken from the patient treatment planning computer: Using single detector, Matrix size is  $1024 \times 1024$  (1.46 zoom), Pixel size is 0.399174 mm. Total count is 50.000.

#### 4.2.2. Intrinsic Spatial Resolution Simulation with GATE

The Monte Carlo code GATE, version 6.2, was used to simulate projection data that set up to describe the thin and thick crystal gamma camera. For ease of computation, a simplified version of the experimental geometry is modelled in the simulation. The result of FWHM of the experiment for the intrinsic spatial resolution is found as 3.33. This number is taken as the reference for the simulation results. In order to get a close result with the experimental value, resolution in the computing program is changed as 2.0 mm, 2.5 mm, 3.0 mm, 3.5 mm and 4.0 mm. In the Figure 4.8, the GATE simulation of the NEMA phantom is illustrated. The count vs energy graph is seen in Figure 4.10.

Figure 4.11 showed how the FWHM has been calculated for the GATE simulation using the ProOrigin program. All the results for the GATE and the experiments are given in Table 4.7 .

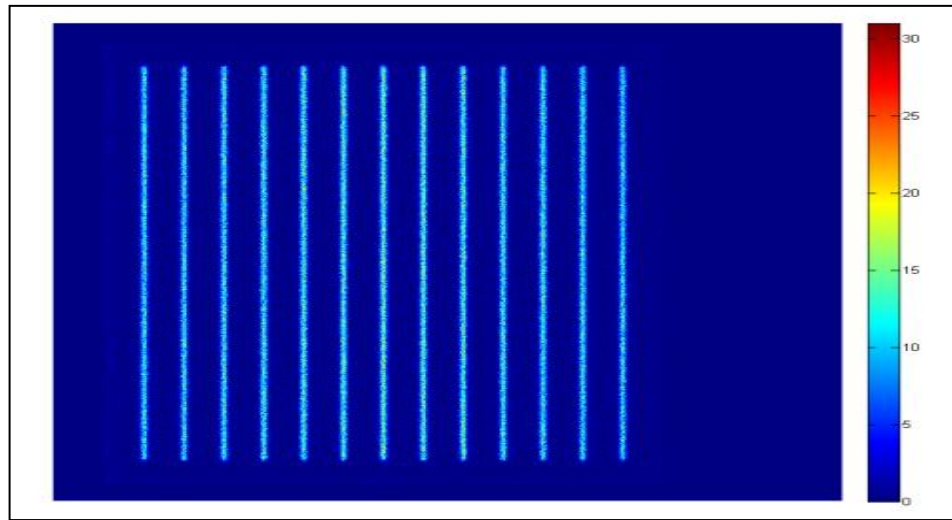


Figure 4.8. Intrinsic spatial resolution for GATE simulation

Experimental value of 3.33 *mm* FWHM corresponds to 3.08 mm intrinsic resolution and this is shown in Figure 4.9.

Table 4.7. Intrinsic Spatial Resolution (NEMA phantom )

Intrinsic Resolution (mm)	Simulation FWHM ( )
2.0	2.22
2.5	2.76
3.0	3.26
3.5	3.76
4.0	4.27



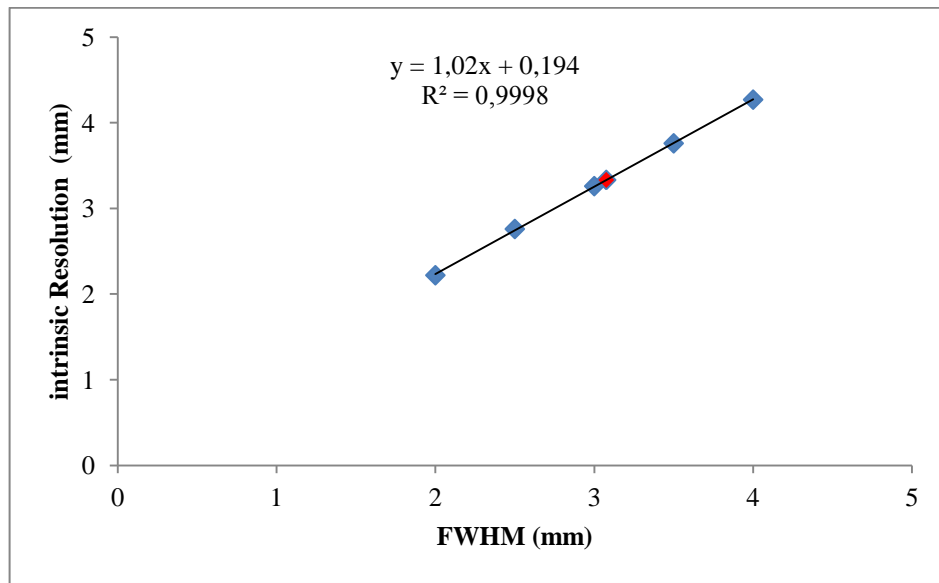


Figure 4.9. Comparison of spatial resolution and fwhm for NEMA collimator

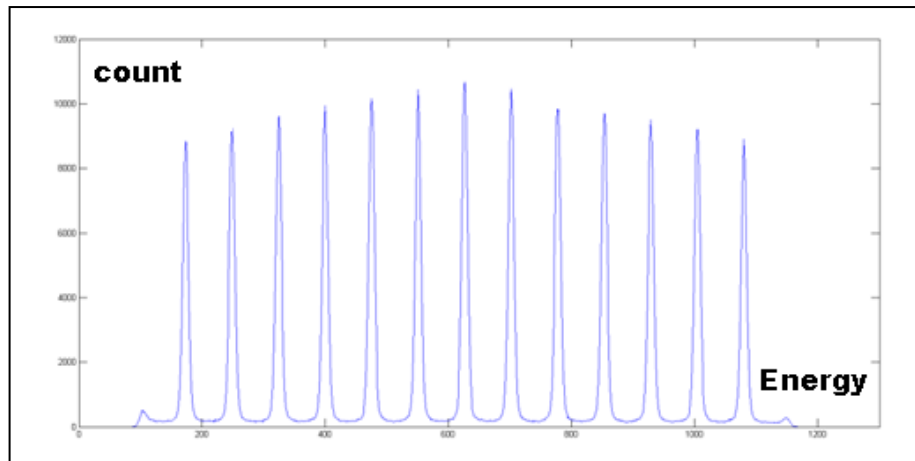


Figure 4.10. Intrinsic resolution as a function of energy for GATE simulation

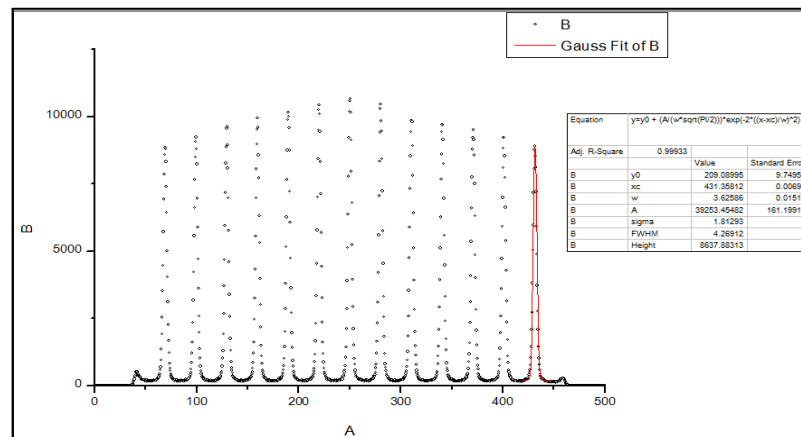


Figure 4.11. FWHM measurement for NEMA phantom for GATE simulation with proOrigin program (count-distance)

#### 4.2.3. Energy Resolution Test

The energy resolution test is done according to the below steps.

- Systems to be tested must be calibrated prior to testing.
- These measurements should be made with an uncollimated detector
- Remove the collimator from the detector being tested.
- Should have 0.700 Ci of  $^{99m}\text{Tc}$  and  $^{57}\text{Co}$  activity amount.
- Place FOV (field of view) mask on the detector.
- Place the  $^{99m}\text{Tc}$  source 2 from the crystal.
- Waiting for three iteration to complete. Then replace the  $^{99m}\text{Tc}$  with a  $^{57}\text{Co}$  source.
- Click the measure  $^{57}\text{Co}$  button. Wait until the energy window disappears.
- The result would be saved.

As a result of all these that calculation of energy resolution is % 9.695 This result is given automatically by the software of the Gamma Camera just offer the test is finished.

#### 4.2.4. Extrinsic Spatial Resolution Experimental Measurement (with VXGP)

Extrinsic spatial resolution test is done according to the below steps.

Procedure :

- Two line sources 10 cm away from each other and 10 cm away from the collimator are used.
- Line sources had internal diameter of 1.5 mm and external diameter 2.5 mm.
- The volume, 0.2 ml, was filled with 1.4 Ci  $^{99m}\text{Tc}$  and the ends of the sources are closed with the parafilm tapes.
- Line sources are placed on VXGP collimator
- The set up is illustrated in Figure ( 4.12- 4.13) .
- Properties of image taken from the patient treatment planning computer: Using single detector, Matrix size is 512×512 (1.46 zoom) , Pixel Size is 0.8 mm , Using activity 1.4 Ci, Total count is 20,000 .

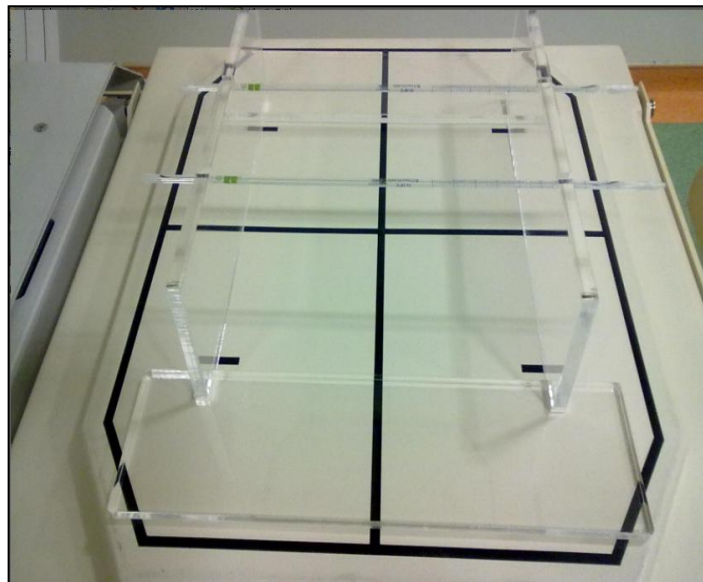


Figure 4.92. Placement of the line sources for the Extrinsic spatial resolution (VXGP)

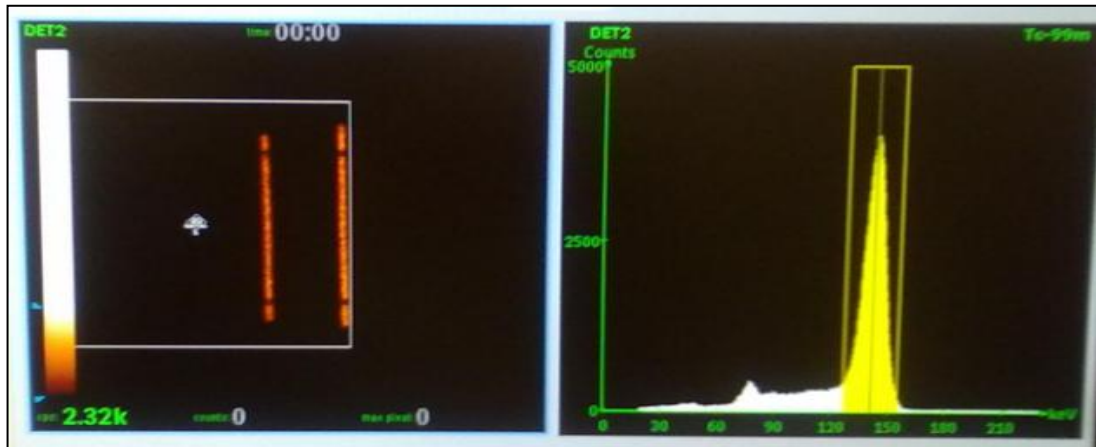


Figure 4.13. Two line Tc-99m source for gamma camera

#### 4.2.5. Extrinsic Spatial Resolution Simulation Measurement (with VXGP)

For the extrinsic spatial resolution determination two line sources of Tc-99m are used. The new sources and their related geometry are installed in the GATE and they are written in APPENDIX D GATE simulation is seen in Figure 4.14 and the results are all give in Table 4.8.

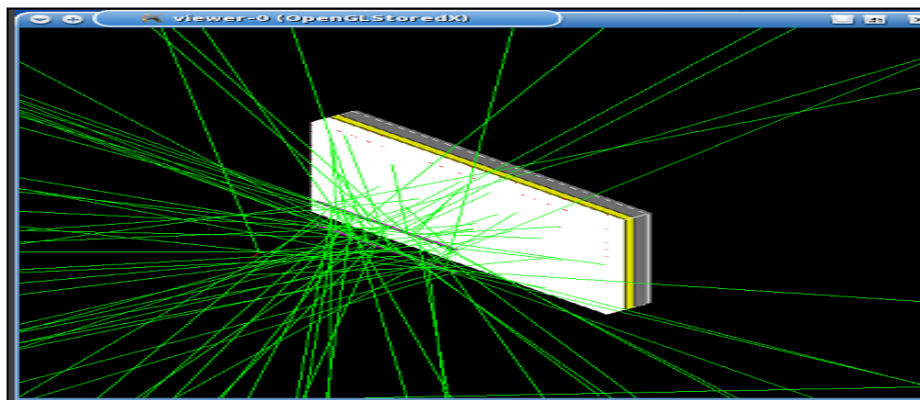


Figure 4.14. GATE simulation for extrinsic spatial resolution test (VXGP)

Extrinsic resolution with the collimator VXGP experimental FWHM value is found as  $7.52 \text{ mm}$  and comparison of spatial resolution and FWHM for VXGP collimator are shown in Figure 4.15.

Table 4.8. Extrinsic spatial resolution- VXGP test results

Resolution ( )	Simulation FWHM ( )	Simulation FWTM ( )
2.0	6.56	11.96
2.5	6.93	12.45
3.0	7.24	13.19
3.5	7.62	13.96
4.0	8.02	14.23

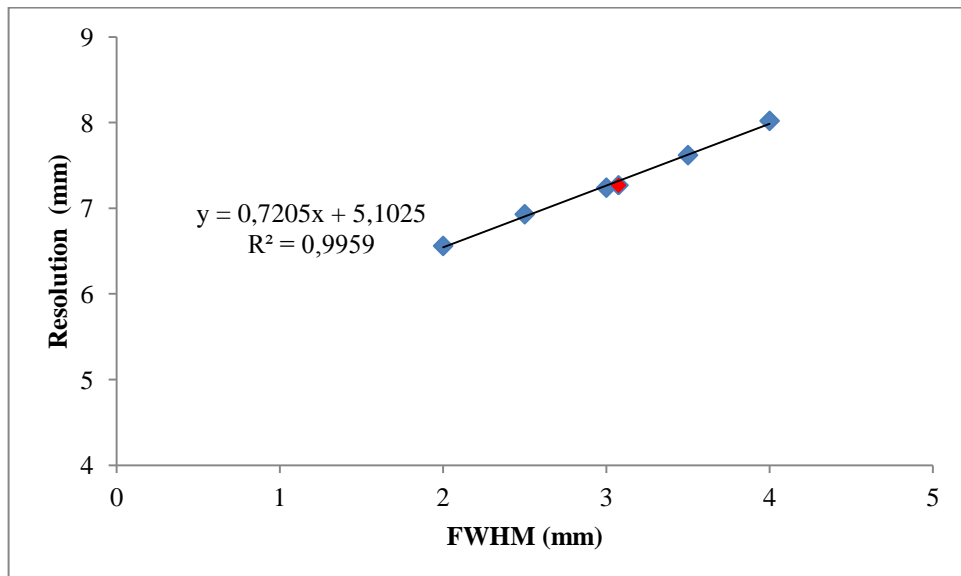


Figure 4.15. Comparison of spatial resolution and FWHM for VXGP collimator

#### 4.2.6. Extrinsic Spatial Resolution - Experimental and Simulation Measurement (with LEGP)

The procedures followed in section 4.2.4 and 4.2.5 are repeated with the collimator LEGP (Low Energy General Purpose). The new geometry of the collimator is induced to GATE program. Collimator and this collimator feature hole shape, size, septa, length, holes number for LEGP were given in Table 4.9 and the results are all give in Table 4.10.

Table 4.9. LEGP specifications

Type	Hole Shape	Size	Septa	Lengh	Holes
Low Energy General Purpose (from now on LEGP)	Hexagon	1.40	0.180	24	86.400

Table 4.10. Extrinsic spatial resolution with LEGP

Resolution ( )	Simulation FWHM ( )	Simulation FWTM ( )
2.0	7.75	14.10
2.5	7.86	14.33
3.0	8.10	14.57
3.5	8.25	14.87
4.0	8.39	15.10

Extrinsic resolution with the collimator LEGP experimental FWHM value is found as 8.26 mm and comparison of spatial resolution and FWHM for LEGP collimator are shown in Figure 4.16.

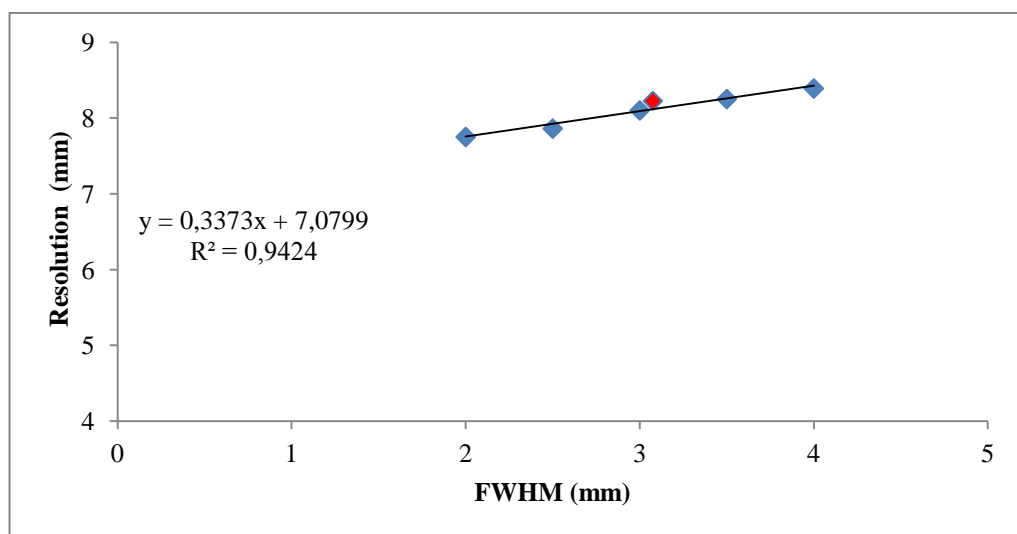


Figure 4.16. Comparison of spatial resolution and FWHM for LEGP collimator

#### 4.2.7. Extrinsic Spatial Resolution Experimental and simulation Measurement with Scattering Medium (with LEGP)

The procedure for the extrinsic spatial resolution test with a scattering medium is as follows,

Procedure :

- Two line sources                      away from each other and 10                      away from the collimator are used.
- Line sources has internal diameter of 1 mm and external diameter 6
- The volume,                      , is filled with                       $^{99m}\text{Tc}$  and the ends of the sources are closed with the parafilm.
- Line sources are placed on LEGP collimator
- Between the line sources a scattering medium is filled. The set up is illustrated in Figure 4.17 and Figure 4.18.
- Properties of image taken from the patient treatment planning computer : Using single dedector, Matrix size is 512×512 (1,46 zoom), Pixel Size is 0.8                      , Using activity is 1.4                      , Total count is 2000                      .

Figure 4.19 Shows Gate simulation for scatter two line source. After doing all the test measurements with the extrinsic spatial resolution with the scattering medium, GATE simulation is changed according to the new collimator LEGP and was run for different resolution values. The results of the GATE simulation are seen in Table 4.11.

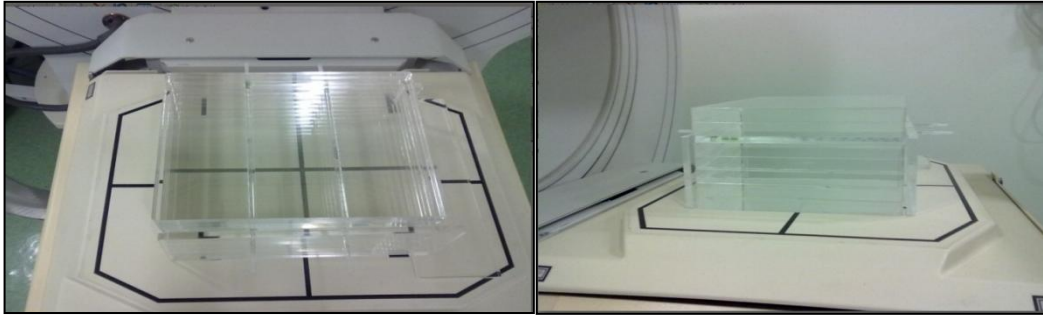


Figure 4.17. Extrinsic test for scattering medium with LEGP collimator.

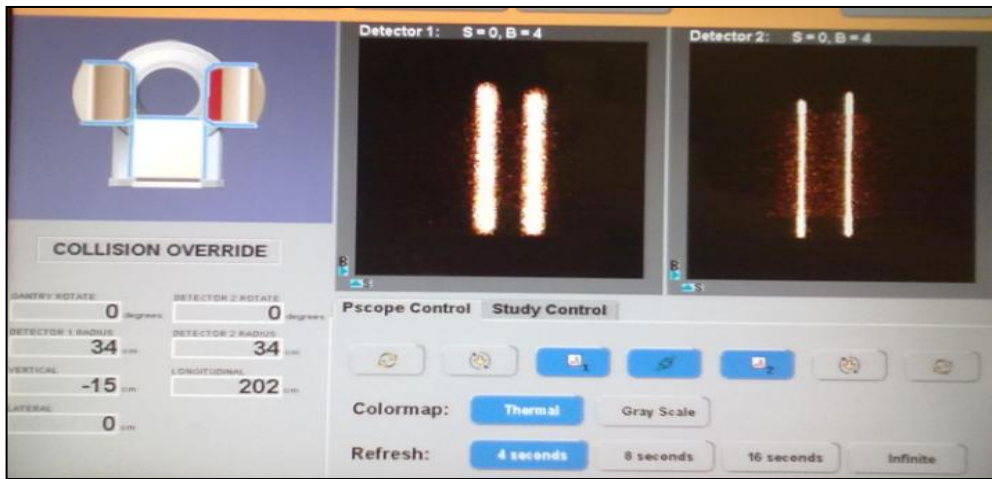


Figure 4.18. With scattering medium for two line source for gamma camera

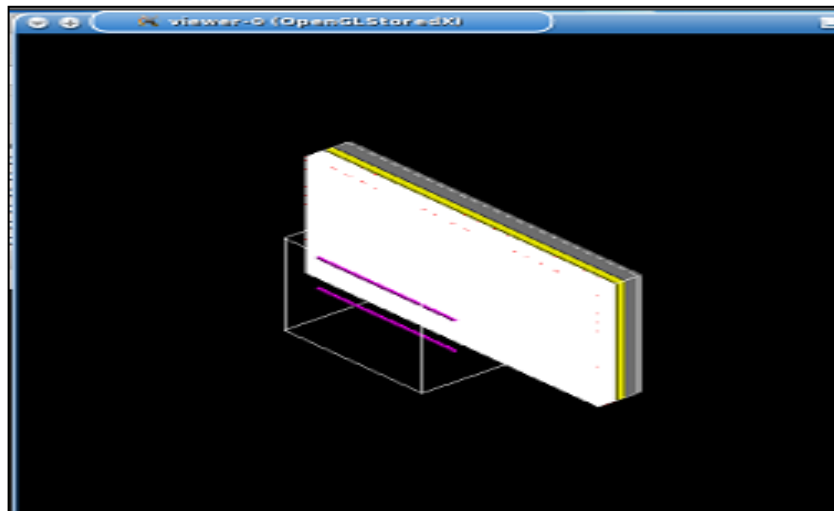


Figure 4.19. Gate simulation for scattering medium for two line source



Table 4.11. Extrinsic spatial resolution scatter LEGP collimator

Resolution ( )	Simulation FWHM ( )	Simulation FWTM ( )
2.0	8.38	15.28
2.5	8.54	15.56
3.0	8.79	16.02
3.5	9.07	16.47
4.0	9.27	16.92

Extrinsic resolution with the collimator LEGP experimental FWHM value is found as 9.42 mm and comparison of spatial resolution scatter and FWHM for LEGP collimator are shown in Figure 4.20.

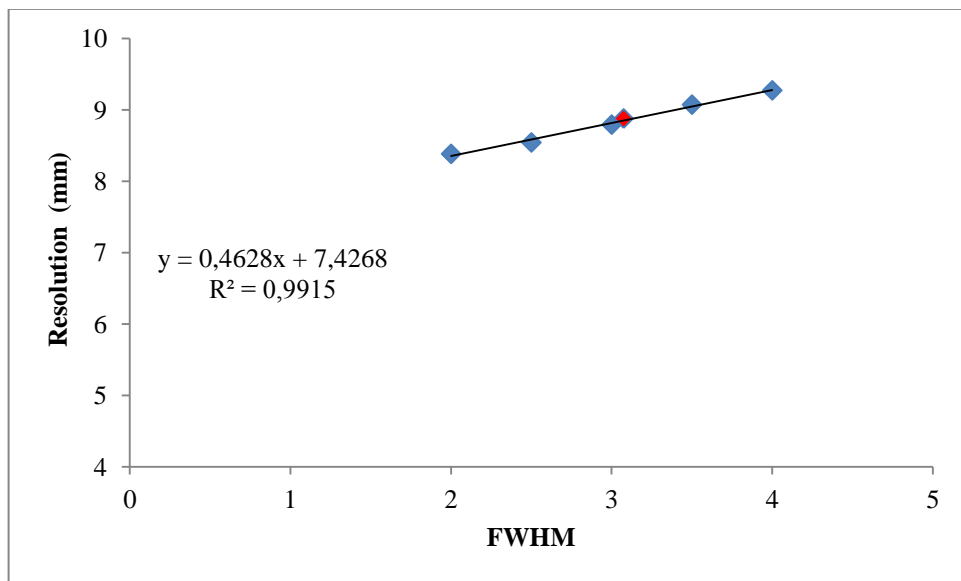


Figure 4.20. Comparison of spatial resolution scatter and FWHM for LEGP collimator

#### 4.2.8. Extrinsic Spatial Resolution Experiment and Simulation Measurement with Scattering Medium (with VXGP)

The procedures followed in section 4.2.7 is repeated with the collimator VXGP (Vertex General purpose). The volume, , is filled with  $^{99m}\text{Tc}$  and the ends of the sources are closed with the parafilm .The new geometry of the collimator is induced to GATE program. Collimator and this collimator feature hole shape, size, septa, length, holes number for VXGP are given in Table 4.12. Extrinsic spatial resolution simulation data with VXGP for phantoms were given in the APPENDIX E.

Extrinsic resolution with the collimator VXGP experimental FWHM value is found as 8.42 mm and comparison of spatial resolution scatter and FWHM for LEGP collimator are shown in Figure 4.21.

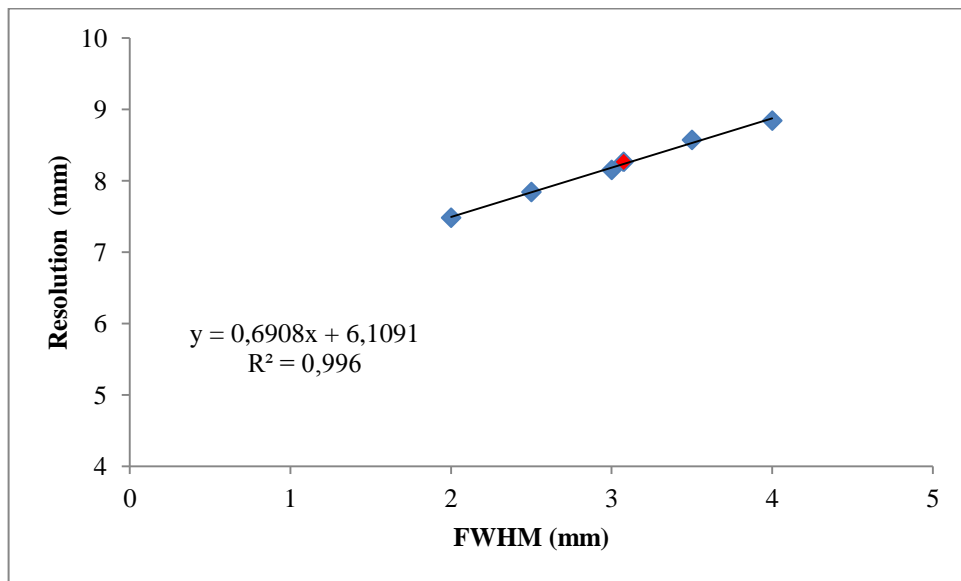


Figure 4.21. Comparison of spatial resolution scatter and fwhm for VGGP collimator

Table 4.12. Extrinsic spatial resolution scatter VXGP collimator

Resolution ( )	Simulation FWHM ( )	Simulation FWTM ( )
2.0	7.48	13.52
2.5	7.84	14.35
3.0	8.15	14.74
3.5	8.57	14.81
4.0	8.84	15.99

#### 4.2.9. Sensitivity Planar Measurement with (LEGP)

The test equipment required for this measurement is                      diameter flat plastic dish filled with an aqueous solution of                       $^{99m}\text{Tc}$ . For different collimator-source distances (                      ), the measurements for the collimator, LEGP was taken according to the regulations. Figures 4.22- 4.24 illustrated all the experimental steps and Sensitivity Planar Measurement result for LEGP as seen in Table 4.13.



Figure 4.22. Sensivity test for distance 5 cm



Figure 4.23. Sensitivity test for distance 40 cm

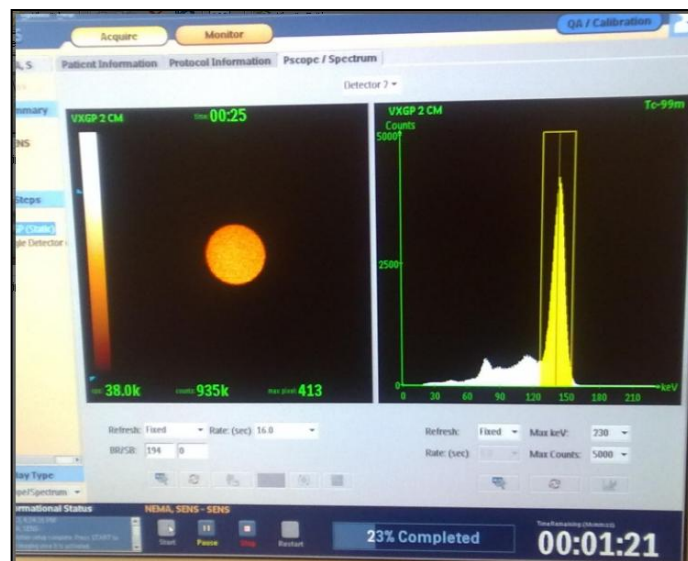


Figure 4.24. Energy spectrum of sensitivity test

Table 4.13 shows measurement for sensitivity planar testing. The flat plastic dish should be filled with water using the large plastic syringe to at least completely cover the bottom of the dish to 2-3 mm depth. The source activity inside the small plastic syringe,  $A_{SR}$ , shall be accurately measured using a dose calibrator. This source shall then be dispersed from this syringe into the flat plastic dish to complete the phantom preparation.

The residual activity remaining in the syringe,  $A_{res}$ , shall be promptly measured in the dose callibrator and the reading subtracted from the original reading to obtain the amount of activity in phantom. Equation 4.1 is the amount of radioactivity measured.  $A_{SR} = 16.05 \text{ mCi}$ ,  $A_{res} = 16.03 \text{ mCi}$ . Equation 4.2 is decay corrected count rate. Total System Sensitivity equation is 4.3.

$$A_{cal} = A_{SR} - A_{res} \quad (4.1)$$

$$R_i = \frac{C_i}{T_{acq,i}} \exp\left(-\lambda(T_i - T_{cal})\right) \quad (4.2)$$

Where,

- $R_i$ : Decay corrected count rate,
- $C_i$ : Count of the  $i$ 'th acquisition,
- $T_i$ : Start time of the  $i$ 'th acquisition,
- $T_{acq,i}$ : Duration of the  $i$ 'th acquisition,
- $T_{cal}$ : Time of the activity calibration,
- $T_{half}$ : Half life of radionuclide (  $21672 \text{ sec}$  for  $Tc-99m$ )

$$\text{Total System Sensitivity} = \frac{R_i}{A_{cal}} \quad (4.3)$$

Total System Sensitivity of PHILIPS-Forte Gamma Camera (LEGP) is 119.36 cps/MBq.

Table 4.13. Measurement for sensitivity planar testing (LEGP)

Collimator - source distance ( )	Total System Sensitivity Calculated (LEGP) (cps/MBq)
2	120.45
5	118,78
10	115.76
15	112.81
20	112.34
25	110.59
30	108.01
35	107.21
40	105.55

## 5. RESULTS & DISCUSSION

The aim of this thesis is to have a detail simulation of Gamma Camera in Yeditepe University Hospital Nuclear Medicine Deapartment to carry the personal dosimetric calculations for all the patients before the treatment.

First of all to get used to the GATE program, different parameters for the gamma camera simulation are changed and the results are shown in Table 4.3-4.6. The changed parameters are activity of the source in NaI crystal as shown in Table 4.3. The YAP crystal thickness is also changed for different activities and are all illustrated in Table 4.4 and Table 4.5. Finally, for one activity of the source the crystals are chosen among the GATE library for the gamma camera as in Table 4.6. The most important part of the GATE simulation is to construct the correct hexagonal geometry of the collimators.

Gamma Camera is a very important instrument and widely used in nuclear medicine. Because of being commonly used, it should be tested regularly. Any problem occurring in any part of the gamma camera should be detected immediately before the decision is made for a case of a patient. The regular tests for this purpose are all given as procedures by NEMA. NEMA acceptance tests are system spatial resolution (intrinsic and extrinsic), sensitivity and energy resolution.

Intrinsic resolution experiment is done by NEMA phantom and the result for the Yeditepe University Hospital gamma camera is found as 3.33 mm FWHM which is convenient with the literature [43]. The GATE model is run for different resolution values because this parameter is set manually for different purposes. The resolution values are given as 2.0, 2.5, 3.0, 3.5 and 4.0 mm and their corresponding simulation FWHM values are shown in Table 4.7. The experimental values of 3.33 mm FWHM corresponds to 3.08 mm intrinsic resolution which is also convenient with the literature [43, 44]. (as seen in Figure 4.9)

Energy resolution experiment for the gamma camera is found as 9.695% and the literature value is 10% at 10cm distance [45,46]. The energy resolution found for our gamma camera as 9.695% is also set in the GATE model for the simulations.

Extrinsic resolution with the collimator VXGP experiment FWHM value is found as 7.52 mm. The GATE simulation results are all shown in Table 4.8 and the 3.08 mm intrinsic resolution corresponding value is calculated as 7.27 mm which has a 3.32 % error with the experimental value (As seen in Figure 4.15). Extrinsic resolution with the collimator LEGP experiment FWHM value is found as 8.26 mm. The GATE simulation results are all shown in Table 4.9 and the 3.08 mm intrinsic resolution corresponding value is calculated as 8.23 mm which has a 0.36 % error with the experimental value (As seen in Figure 4.16).

In the above experiments the sources are not in a scattering medium, but if we think of a patient, the source is in the body and the body is a scattering medium. A plastic medium is built around the sources and the extrinsic resolution tests are all repeated with the new setup. Extrinsic resolution with the collimator LEGP experiment FWHM value is found as 9.42 mm. The GATE simulation results are all shown in Table 4.11 and the 3.08 mm intrinsic resolution corresponding value is calculated as 8.88 mm which has a 5.73 % error with the experimental value (as seen in Figure 4.20). The GATE simulation values for the FWTM changes more because of the scattering medium. In the scattering medium, the count vs distance graphs have broadening shapes at the low counts. Extrinsic resolution with the collimator VXGP experiment FWHM value is found as 8.42 mm. The GATE simulation results are all shown in Table 4.12 and the 3.08 mm intrinsic resolution corresponding value is calculated as 8.26 mm which has a 1.90 % error with the experimental value (as seen in Figure 4.21) .

The sensitivity of the gamma camera is calculated as 115.76 cps/MBq . The result show that difference between the calculated and given specification of PHILIPS-Forte Gamma Camera values differ by 3.02 %. In the literature, expect range of each collimator combination is < 5 % [43, 47, 48].



In the literature at 10 cm, the gamma camera resolution is taken as 15mm. [45, 46] The simulations and the experiments show that our gamma camera resolution values are all compatible with the literature.

## **6. CONCLUSION AND FUTURE WORK**

Every acceptance test for the gamma camera of Yeditepe University have been done. Routinely used PHILIPS-Forte Gamma Camera is working properly. The GATE simulation is done successfully and is ready for different purpose of use. The next step of this study is to have a voxelized phantom of the patient from the computerized tomography images and to make a personal dosimetry for all the patients before the treatment. We expect to make the personal dosimetry a must before the activity treatment of the patient.

## 7. REFERENCES

1. <http://www.opengatecollaboration.org/Documentation>
2. Benoit, D., *GATE Training*, 2012.
3. Carlo, Monte. <http://www.puc-rio.br/marco.ind/monte-carlo.html>.
4. Wagenaar, D., M. Kapusta, J. Li, and B. Patt, *Rationale for the combination of nuclear medicine with magnetic resonance for pre-clinical imaging.*, pp. 343–350, 2006.
5. Guy, C., *An Introduction to The Principles of Medical Imaging*, London, UK, 2005.
6. Knoll, G., "Radiation Detection and Measurement, 3rd Edit John Wiley & Sons, 2000.
7. Gordon, G., *Practical Gamma-ray Spectrometry*(pp.33-34), 1995.
8. Dağ, Y., Gama kamera ve çalışma prensipleri.
9. Al-Gholeeqah, A., and K. Yousef, *Nuclear Medicine and Gamma Camera*, pp.45-47
10. Sahoo, S., "Production and Applications of Gamma", 2006.
11. IAEA,. <http://nucleus.iaea.org/2013>.
12. Knoll, G. F., *Radiation Detection and Measurement*, 2nd ed., 1989.
13. Iniewski, K., *Medical Imaging-Principles, Detectors, and Electronics*, pp.104

14. Demir, M., *Nükleer Tıp Fiziği ve Klinik uygulamaları*, 3rd ed.
15. <http://backreaction.blogspot.com/2008/11/technetium-99.html>
16. Bronstein A., M. Bronstein, M. Zibulevsky and Y. Y. Zeevi, "High-Energy Photon Detection in Positron Emission Tomography Using Adaptive Non-Linear Parametric Estimation Algorithms", Technion – Israel Institute of Technology Department of Electrical Engineering, the Vision Research and Image Science Laboratory, technical report, 2002.
17. Ahmed, S., *Physics and Engineering of Radiation Detection.*, Elsevier Academic Press, Amsterdam, The Netherlands, 2007.
18. Suetens, P., *Fundamentals of Medical Imaging (Pp 105-116)*, Cambridge University Press 2009.
19. Frans van der, H., B. Vastenhov, M. Rentmeester. (July 2008) System Calibration and Statistical Image Reconstruction for Ultra-High Resolution Stationary Pinhole SPECT.
20. Cherry, S., J. Sorensen, and M. Phelps, *Physics in Nuclear Medicine*, Philadelphia, Pennsylvania, 2003.
21. Buzhan, P., B. Dolgoshein, L. Filatov, A. Ilyin, V. Kaplin, A. Karakash, *Large area silicon photomultipliers: Performance and applications.*, Large area silicon photomultipliers: Performance and applications. Nuclear Instruments and Methods in Physics Research (78–82), 2006.
22. Tao, Ashley T., *Development of a Silicon Photomultiplier Based*, 4-1-2012.
23. Buxton, R., *Introduction to Functional Magnetic Resonance Imaging*, Cambridge

University Press, 2009.

24. Hamamatsu, K., *Photomultiplier tubes Basics and Applications, 3rd edition*”, 2007.
26. Ljungberg, M., S.E Strand and M.A. King, *Monte Carlo Calculations in Nuclear Medicine*, UK, Bristol : J.W Arrowsmith, 1998.
27. Simulation, Small Animal PET and Monte Carlo. <http://www.org.chemie.tu-muenchen.de/people/fhagn/JASS2006/files/JASS2006-Torres-Espallardo.pdf>.
28. Simulations of Preclinical and Clinical Scans in Emission Tomography, Transmission Tomography and Radiation Therapy. <http://www.opengatecollaboration.org/>.
29. Andreyev, A., Dual-isotope Pet Using Positron-Gamma Emitters, 2011, 1 July.
30. Erturk, SS., *Optimization of the Parameters of The YAP-(S)PETII Scanner*, 2008-2010.
31. Grevillot, L., Simulation of a 6MV Elekta Precise Linac Photon beam using GATE/GEANT, 2011.
32. H. H, Barrett., and W. Swindell, *Radiological Imaging. The Theory of Image Formation, Detection and Processing*, New York, USA, (438–439), 1981.
33. Hammes1, J., "GATE based Monte Carlo simulation of planar scintigraphy to", *ORIGINALARBEIT*, 2011.
34. Assie, K., I. Gardin, P. Vera and I. buvat. Validation of Monte Carlo simulator GATE for indium-111 imaging, 2005.

35. Maigne, L., Y.Perrot ,D. R. schart, D. Donnarieix and V. Breton. Comparison of GATE/GEANT+ with EGSnrc and MCNP for electron dose calculations at energies between 15 keV and 20 MeV, 14 January 2011.
36. Morel, C., GATE: a simulation toolkit for PET and SPECT, 2004.
37. Jan, S., D. Benoit, E. Becheva, T.Carlier, F. cassol, P. Descourt, T. Frisson, L.Grevillot, Lguigues, L. Maigne, C. Morel, Y.Perrot, N. Rehfeld, D.Sarrut, D. R.Schaart,S.Stute,U. Pietrzyk, D. Visvikis, N. Zahre and I. Buvat. GATE V6:a major anhancement of the GATE simulation platform enabling modelling of CT and radiotherapy.
38. Sharp, Professor P.F.Course., *Department of Biomedical Physics*, Session, 2003 -2004.
39. Powsner, Rachel A., and R.Powsner-Edward, *Essential Nuclear medicine Physics*, 2nd ed.
40. Pietrzyk, U., "basic examples for educative purpose using the", pp. 6, ZEMEDI, 2012.
41. Wernick, M., and J. Aarsvold, *Emission Tomography: The Fundamentals of PET and SPECT*, Elsevier Academic Press, 2004.
42. William R, H., *MEDICAL*, 4th ed., A JOHN WILEY & SONS, INC., PUBLICATION
43. Staelens, S., and D. Strul and G. Santin , Monte Carlo simulation of a scintillation camera using GATE, 2003.
44. Elshemey W, M., Scattered radiation effects on the extrinsic sensitivity and counting efficiency of a gamma camera, 2012.
45. A, Karine., Monte Carlo simulation in PET and SPECT instrumentation using GATE, 2004.

46. Holstensson, M., M. Partridge, S. Buckley and G. Flux, The effect of energy and source location on gamma camera intrinsic and extrinsic spatial resolution: an experimental and Monte Carlo, 2009.

47. M, Momenzhad ., Development of GATE Monte Carlo simulation for a dual-head gamma camera, 2011.

48. J, Halama., PhD Nuclear Medicine Physicist Loyola University Medical Center

<http://www.medphysics.wisc.edu/courses/mp573/NM%3FPET%20radlab/HalamaSlides.pdf>

## APPENDIX A: PRACTICE THE BUILDING GATE OF 8 STEPS

```

/gate/holeg1/cubicArray/setRepeatNumberY 84
/gate/holeg1/cubicArray/setRepeatNumberZ 1
/gate/holeg1/cubicArray/setRepeatVector 0.774 0.447 0. cm
/gate/holeg1/repeaters/insert linear
/gate/holeg1/linear/setRepeatNumber 2
/gate/holeg1/linear/setRepeatVector 0.387 0.2235 0. cm
Physics list
Define particles
/gate/physics/addProcess IonInelastic alpha
Define physics processes
/gate/physics/addProcess PhotoElectric
/gate/physics/addProcess Compton
/gate/physics/addProcess GammaConversion
/gate/physics/addProcess ElectronIonisation
/gate/physics/addProcess Bremsstrahlung
/gate/physics/addProcess PositronAnnihilation
/gate/physics/addProcess MultipleScattering e+
/gate/physics/addProcess MultipleScattering e-
The sources
General Particle Sources
Model simple emission geometries
Can generate particles or ions
User must define
total activity
emission geometry
Direction, energy
For example,
/gate/source/addSource fluor18
/gate/source/fluor18/setActivity 5. becquerel
/gate/source/fluor18/gps/particle ion
/gate/source/fluor18/gps/ion 9 18 0 0
/gate/source/fluor18/gps/energytype Mono
/gate/source/fluor18/gps/monoenergy 0. MeV
/gate/source/fluor18/gps/angtype iso
/gate/source/fluor18/gps/number 1
/gate/source/fluor18/gps/centre 0. 0. 0. cm
/gate/source/fluor18/gps/type Volume

```



```
/gate/source/fluor18/gps/shapeSphere
/gate/source/fluor18/gps/radius 1. mm
/gate/source/fluor18/gps/confine head_P
For example for a block detector,
# BLOCK
/gate/module/daughters/name block
/gate/module/daughters/insert box
# C R Y S T A L
/gate/block/daughters/name crystal
/gate/block/daughters/insert box
/gate/crystal/placement/setTranslation 0.0 0.0 0.0 cm
/gate/crystal/geometry/setXLength 3.0 cm
/gate/crystal/geometry/setYLength 3.0 mm
/gate/crystal/geometry/setZLength 3.8 mm
/gate/crystal/setMaterial Air
/gate/crystal/vis/setVisible 0
# R E P E A T C R Y S T A L
/gate/crystal/repeaters/insert cubicArray
/gate/crystal/cubicArray/setRepeatNumberX 1
/gate/crystal/cubicArray/setRepeatNumberY 5
/gate/crystal/cubicArray/setRepeatNumberZ 5
/gate/crystal/cubicArray/setRepeatVector 0.0 3.2 4.0 mm
# R E P E A T BLOCK
/gate/block/repeaters/insert cubicArray
/gate/block/cubicArray/setRepeatNumberX 1
/gate/block/cubicArray/setRepeatNumberY 8
/gate/block/cubicArray/setRepeatNumberZ 12
/gate/block/cubicArray/setRepeatVector 0.0 1.6 2.0 cm
```

## APPENDIX B: MY GAMMA CAMERA CODES FOR CYLINDRICAL PHANTOM

```
# V I S U A L I S A T I O N
#####
#/vis/disable
/control/execute vis.mac
# M A N D A T O R Y
#####
/gate/geometry/setMaterialDatabase GateMaterials.db
# G E O M E T R Y
#####
# World
# Define the world dimensions
##
/gate/world/geometry/setXLength 200 cm
/gate/world/geometry/setYLength 200 cm
/gate/world/geometry/setZLength 200 cm
# Scanner Head
# Create a new box representing the main head-volume
# SPECThead is the name of the predefined SPECT system
# Create the SPECT system, which will yield an Interfile output
of projection data
/gate/world/daughters/name SPECThead
/gate/world/daughters/insert box
/gate/SPECThead/geometry/setXLength 8. cm
/gate/SPECThead/geometry/setYLength 42. cm
/gate/SPECThead/geometry/setZLength 55. cm
/gate/SPECThead/placement/setTranslation 20.0 0. 0. cm
/gate/SPECThead/setMaterial Air
/gate/SPECThead/vis/forceWireframe
```

```
# Collimator
# Create a full volume defining the shape of the collimator
/gate/SPECThead/daughters/name collimator
/gate/SPECThead/daughters/insert box
/gate/collimator/geometry/setXLength 4.2 cm
/gate/collimator/geometry/setYLength 42. cm
/gate/collimator/geometry/setZLength 55. cm
/gate/collimator/placement/setTranslation -1.9 0. 0. cm
/gate/collimator/setMaterial Lead
/gate/collimator/vis/setColor red
/gate/collimator/vis/forceWireframe
#
# Insert the first hole of air in the collimator
##
/gate/collimator/daughters/name hole
/gate/collimator/daughters/insert hexagone
/gate/hole/geometry/setHeight 4.2 cm
/gate/hole/geometry/setRadius 0.089 cm
/gate/hole/placement/setRotationAxis 0 1 0
/gate/hole/placement/setRotationAngle 90 deg
/gate/hole/setMaterial Air
#
# Repeat the hole in an array
##
/gate/hole/repeaters/insert cubicArray
/gate/hole/cubicArray/setRepeatNumberX 1
/gate/hole/cubicArray/setRepeatNumberY 227
/gate/hole/cubicArray/setRepeatNumberZ 172
/gate/hole/cubicArray/setRepeatVector 0. 0.185 0.320 cm
# Repeat these holes in a linear
##
/gate/hole/repeaters/insert linear
/gate/hole/linear/setRepeatNumber 2
/gate/hole/linear/setRepeatVector 0. 0.0925 0.160 cm
# CRYSTAL
# Create the crystal volume
```

```
/gate/SPECThead/daughters/name crystal
/gate/SPECThead/daughters/insert box
/gate/crystal/geometry/setXLength 0.95 cm
/gate/crystal/geometry/setYLength 42. cm
/gate/crystal/geometry/setZLength 55. cm
/gate/crystal/placement/setTranslation 0.675 0. 0. cm
/gate/crystal/setMaterial NaI
/gate/crystal/vis/forceSolid
/gate/crystal/vis/setColor yellow
# BACK-COMPARTMENT
# Create the back-compartment volume
/gate/SPECThead/daughters/name compartment
/gate/SPECThead/daughters/insert box
/gate/compartment/geometry/setXLength 2.5 cm
/gate/compartment/geometry/setYLength 42. cm
/gate/compartment/geometry/setZLength 55. cm
/gate/compartment/placement/setTranslation 2.4 0. 0. cm
/gate/compartment/setMaterial Glass
/gate/compartment/vis/forceSolid
/gate/compartment/vis/setColor grey
# TABLE
# Create the table volume
/gate/world/daughters/name table
/gate/world/daughters/insert box
/gate/table/geometry/setXLength 25. cm
/gate/table/geometry/setYLength 1.5 cm
/gate/table/geometry/setZLength 160. cm
/gate/table/placement/setTranslation 0. -5.75 0. cm
/gate/table/setMaterial Glass
/gate/table/vis/forceSolid
/gate/table/vis/setColor white
/gate/world/daughters/name Phantom
```

```
/gate/world/daughters/insert cylinder
/gate/Phantom/geometry/setRmax 2. cm
/gate/Phantom/geometry/setRmin 0. cm
/gate/Phantom/geometry/setHeight 5. cm
/gate/Phantom/placement/setTranslation 0. 0. 0. cm
/gate/Phantom/setMaterial Water
/gate/Phantom/vis/forceSolid
/gate/Phantom/vis/setColor magenta
# S Y S T E M
# The system acts as an interpreter between the GATE geometry
and data outputs for reconstruction
# in our case, the Interfile writer
# A system must know which components of the geometry are parts
of the scanner, and what
# their role are.
# For the moment, there is only a system SPECThead, which was
built when the SPECThead volume
# was inserted.
# The SPECThead system is made of three levels: base (for the
head), crystal (for the crystal and crystal matrix)
# and pixel (for individual crystals for pixellated gamma
camera)
# For now, only the base of the system is attached to a volume:
the volume SPECThead
# For the system to get information about your crystal, the
level crystal must be attached to the volume
# that has been defined for the scintillating crystal (crystal)
##
/gate/systems/SPECThead/crystal/attach crystal
/gate/systems/SPECThead/describe
```

```

# S E N S I T I V E   D E T E C T O R S
# Using them properly is very important for getting accurate
results
##
# Crystal SD
# The crystal SD makes it possible to record hits in a
sensitive volume (e.g.,. in a scintillation crystal)
# It must be attached to any volume for which hit-data must be
obtained

# For recording hits in the NaI volume only, the name of which
is crystal, this volume is attached
# to the crystal SD
##
/gate/crystal/attachCrystalSD
# Phantom SD#
# The phantom SD makes it possible to record Compton events in
the volumes within the field of view
# This can provide information for result analysis to
discriminate between
# scattered and unscattered photons
# It must be attached to each and every volume for whom Compton
interactions have to be recorded
##
/gate/Phantom/attachPhantomSD
/gate/table/attachPhantomSD
/gate/compartment/attachPhantomSD
/gate/SPECThead/attachPhantomSD
/gate/collimator/attachPhantomSD
# P H Y S I C S
/gate/physics/addProcess PhotoElectric
/gate/physics/processes/PhotoElectric/setModel StandardModel
/gate/physics/addProcess Compton
/gate/physics/processes/Compton/setModel PenelopeModel
/gate/physics/addProcess RayleighScattering
/gate/physics/processes/RayleighScattering/setModel
PenelopeModel
/gate/physics/addProcess ElectronIonisation

```

```
/gate/physics/processes/ElectronIonisation/setModel
StandardModel e-
/gate/physics/addProcess Bremsstrahlung
/gate/physics/processes/Bremsstrahlung/setModel StandardModel
e-

/gate/physics/processList Initialized
# C U T S
#####
# Cuts for particle in WORLD
##
/gate/physics/Gamma/SetCutInRegion      SPECThead 0.1 cm
/gate/physics/Electron/SetCutInRegion   SPECThead 1.0 cm
# I N I T I A L I Z A T I O N
#####
/gate/run/initialize
/control/execute secondPart.mac
```

**APPENDIX C: LINE SOURCE FOR VXGP COLLIMATOR**

```
# V I S U A L I S A T I O N
#####
/vis/enable
#/control/execute MoveVisu.mac
# M A N D A T O R Y
#####
/gate/geometry/setMaterialDatabase GateMaterials.db
# G E O M E T R Y
#####
# World
# Define the world dimensions
##
/gate/world/geometry/setXLength 600 cm
/gate/world/geometry/setYLength 600 cm
/gate/world/geometry/setZLength 600 cm
# Scanner Head
# Create a new box representing the main head-volume
# SPECThead is the name of the predefined SPECT system
# Create the SPECT system, which will yield an Interfile output
of projection data
##
/gate/world/daughters/name SPECThead
/gate/world/daughters/insert box
/gate/SPECThead/geometry/setXLength 8. cm
/gate/SPECThead/geometry/setYLength 38.1 cm
/gate/SPECThead/geometry/setZLength 50.8 cm
/gate/SPECThead/placement/setTranslation 0. 0. 0. cm
/gate/SPECThead/setMaterial Air
/gate/SPECThead/vis/forceWireframe
/gate/SPECThead/attachPhantomSD
# Collimator
# Create a full volume defining the shape of the collimator
```



```

/gate/SPECThead/daughters/name collimator
/gate/SPECThead/daughters/insert box
/gate/collimator/geometry/setXLength 4.2 cm
/gate/collimator/geometry/setYLength 38.1 cm
/gate/collimator/geometry/setZLength 50.8 cm
/gate/collimator/placement/setTranslation -1.9 0. 0. cm
/gate/collimator/setMaterial Lead
/gate/collimator/vis/setColor red
/gate/collimator/vis/forceWireframe
/gate/collimator/attachPhantomSD
#
# Insert the first hole of air in the collimator
##
/gate/collimator/daughters/name hole
/gate/collimator/daughters/insert hexagone
/gate/hole/geometry/setHeight 4.2 cm
/gate/hole/geometry/setRadius 0.089 cm
/gate/hole/placement/setRotationAxis 0 1 0
/gate/hole/placement/setRotationAngle 90 deg
/gate/hole/setMaterial Air
/gate/hole/attachPhantomSD
#
# Repeat the hole in an array
##
/gate/hole/repeaters/insert cubicArray
/gate/hole/cubicArray/setRepeatNumberX 1
/gate/hole/cubicArray/setRepeatNumberY 206
/gate/hole/cubicArray/setRepeatNumberZ 159
/gate/hole/cubicArray/setRepeatVector 0. 0.185 0.320 cm
#
# Repeat these holes in a linear
##
/gate/hole/repeaters/insert linear
/gate/hole/linear/setRepeatNumber 2
/gate/hole/linear/setRepeatVector 0. 0.0925 0.160 cm
# CRYSTAL
# Create the crystal volume

```

```

/gate/SPECThead/daughters/name crystal
/gate/SPECThead/daughters/insert box
/gate/crystal/geometry/setXLength 0.95 cm
/gate/crystal/geometry/setYLength 38.1 cm
/gate/crystal/geometry/setZLength 50.8 cm
/gate/crystal/placement/setTranslation 0.675 0. 0. cm
/gate/crystal/setMaterial NaI
/gate/crystal/vis/forceSolid
/gate/crystal/vis/setColor yellow
/gate/crystal/attachCrystalSD
# BACK-COMPARTMENT
# Create the back-compartment volume
##
/gate/SPECThead/daughters/name compartment
/gate/SPECThead/daughters/insert box
/gate/compartment/geometry/setXLength 2.5 cm
/gate/compartment/geometry/setYLength 38.1 cm
/gate/compartment/geometry/setZLength 50.8 cm
/gate/compartment/placement/setTranslation 2.4 0. 0. cm
/gate/compartment/setMaterial Glass
/gate/compartment/vis/forceSolid
/gate/compartment/vis/setColor grey
/gate/compartment/attachPhantomSD
# Phantom
#
##
/gate/world/daughters/name Phantom
/gate/world/daughters/insert cylinder
/gate/Phantom/geometry/setRmax 3. mm
/gate/Phantom/geometry/setRmin 0.5 mm
/gate/Phantom/geometry/setHeight 24. cm
#/gate/Phantom/placement/setRotationAxis 1 0 0
#/gate/Phantom/placement/setTranslation -14. 0. 5. cm
/gate/Phantom/placement/setTranslation -14. 5. 0. cm
/gate/Phantom/setMaterial Glass
/gate/Phantom/vis/forceSolid
/gate/Phantom/vis/setColor magenta
/gate/Phantom/attachPhantomSD

```

```

/gate/world/daughters/name Phantom2
/gate/world/daughters/insert cylinder
/gate/Phantom2/geometry/setRmax 3. mm
/gate/Phantom2/geometry/setRmin 0.5 mm
/gate/Phantom2/geometry/setHeight 24. cm
#/gate/Phantom2/placement/setRotationAxis 1 0 0
#/gate/Phantom2/placement/setTranslation -14. 0. -5. cm
/gate/Phantom2/placement/setTranslation -14. -5. 0. cm
/gate/Phantom2/setMaterial Glass
/gate/Phantom2/vis/forceSolid
/gate/Phantom2/vis/setColor magenta
/gate/Phantom2/attachPhantomSD

# S Y S T E M
# The system acts as an interpretor between the GATE geometry
and data outputs for reconstruction
# in our case, the Interfile writer
# A system must know which components of the geometry are parts
of the scanner, and what
# their role are.
# For the moment, there is only a system SPECThead, which was
built when the SPECThead volume
# was inserted.
# The SPECThead system is made of three levels: base (for the
head), crystal (for the crystal and crystal matrix)
# and pixel (for individual crystals for pixellated gamma
camera)
# For now, only the base of the system is attached to a volume:
the volume SPECThead
# For the system to get information about your crystal, the
level crystal must be attached to the volume
# that has been defined for the scintillating crystal (crystal)
/gate/systems/SPECThead/crystal/attach crystal
/gate/systems/SPECThead/describe

# S E N S I T I V E   D E T E C T O R S
# GATE provides two sensitive detectors, which have two
different functions
# Using them properly is very important for getting accurate
results
# Crystal SD

```

```
## The crystal SD makes it possible to record hits in a
sensitive volume (e.g.,. in a scintillation crystal)
# It must be attached to any volume for which hit-data must be
obtained
# For recording hits in the NaI volume only, the name of which
is crystal, this volume is attached
# to the crystal SD

/gate/crystal/attachCrystalSD
# P H Y S I C S
/gate/physics/addProcess LowEnergyPhotoElectric
/gate/physics/addProcess LowEnergyCompton
/gate/physics/addProcess LowEnergyRayleighScattering
/gate/physics/addProcess ElectronIonisation
/gate/physics/addProcess Bremsstrahlung
/gate/physics/addProcess MultipleScattering e-
/gate/physics/processList Enabled
/gate/physics/processList Initialized
# C U T S
# Cuts for particle in WORLD
/gate/physics/Gamma/SetCutInRegion      SPECThead 0.1 cm
/gate/physics/Electron/SetCutInRegion   SPECThead 1.0 cm
/gate/run/initialize
# I N I T I A L I Z A T I O N
/control/execute secondPart_LineSources_X.mac
```

## APPENDIX D: EXTRINSIC SPATIAL RESOLUTION SIMILATION DATA WITH VXGP FOR PHANTOMS

```
# Phantom
/gate/world/daughters/name Phantom
/gate/world/daughters/insert cylinder
/gate/Phantom/geometry/setRmax 3. mm
/gate/Phantom/geometry/setRmin 0.5 mm
/gate/Phantom/geometry/setHeight 24. cm
#/gate/Phantom/placement/setRotationAxis 1 0 0
#/gate/Phantom/placement/setTranslation -14. 0. 5. cm
/gate/Phantom/placement/setTranslation -14. 5. 0. cm
/gate/Phantom/setMaterial Glass
/gate/Phantom/vis/forceSolid
/gate/Phantom/vis/setColor magenta
/gate/Phantom/attachPhantomSD

/gate/world/daughters/name Phantom2
/gate/world/daughters/insert cylinder
/gate/Phantom2/geometry/setRmax 3. mm
/gate/Phantom2/geometry/setRmin 0.5 mm
/gate/Phantom2/geometry/setHeight 24. cm
#/gate/Phantom2/placement/setRotationAxis 1 0 0
#/gate/Phantom2/placement/setTranslation -14. 0. -5. cm
/gate/Phantom2/placement/setTranslation -14. -5. 0. cm
/gate/Phantom2/setMaterial Glass
/gate/Phantom2/vis/forceSolid
/gate/Phantom2/vis/setColor magenta
/gate/Phantom2/attachPhantomSD
```

**APPENDIX E: VXGP SCATTER EXTRINSIC TEST CODES**

```
# V I S U A L I S A T I O N
#####
/vis/disable
#/control/execute vis.mac
# M A N D A T O R Y
#####
/gate/geometry/setMaterialDatabase GateMaterials.db
# G E O M E T R Y
#####
# World
# Define the world dimensions
##
/gate/world/geometry/setXLength 600 cm
/gate/world/geometry/setYLength 600 cm
/gate/world/geometry/setZLength 600 cm
# Scanner Head
# Create a new box representing the main head-volume
# SPECThead is the name of the predefined SPECT system
# Create the SPECT system, which will yield an Interfile output
of projection data
##
/gate/world/daughters/name SPECThead
/gate/world/daughters/insert box
/gate/SPECThead/geometry/setXLength 8. cm
/gate/SPECThead/geometry/setYLength 38.1 cm
/gate/SPECThead/geometry/setZLength 50.8 cm
/gate/SPECThead/placement/setTranslation 0. 0. 0. cm
/gate/SPECThead/setMaterial Air
/gate/SPECThead/vis/forceWireframe
# Collimator
# Create a full volume defining the shape of the collimator
```

```
/gate/SPECThead/daughters/name collimator
/gate/SPECThead/daughters/insert box
/gate/collimator/geometry/setXLength 4.2 cm
/gate/collimator/geometry/setYLength 38.1 cm
/gate/collimator/geometry/setZLength 50.8 cm
/gate/collimator/placement/setTranslation -1.9 0. 0. cm
/gate/collimator/setMaterial Lead
/gate/collimator/vis/setColor red
/gate/collimator/vis/forceWireframe
# Insert the first hole of air in the collimator
/gate/collimator/daughters/name hole
/gate/collimator/daughters/insert hexagone
/gate/hole/geometry/setHeight 4.2 cm
/gate/hole/geometry/setRadius 0.0089 cm
/gate/hole/placement/setRotationAxis 0 1 0
/gate/hole/placement/setRotationAngle 90 deg
/gate/hole/setMaterial Air
# Repeat the hole in an array
/gate/hole/repeaters/insert cubicArray
/gate/hole/cubicArray/setRepeatNumberX 1
/gate/hole/cubicArray/setRepeatNumberY 206
/gate/hole/cubicArray/setRepeatNumberZ 159
/gate/hole/cubicArray/setRepeatVector 0. 0.185 0.320 cm
# Repeat these holes in a linear
/gate/hole/repeaters/insert linear
/gate/hole/linear/setRepeatNumber 2
/gate/hole/linear/setRepeatVector 0. 0.0925 0.160 cm
# CRYSTAL
# Create the crystal volume
/gate/SPECThead/daughters/name crystal
/gate/SPECThead/daughters/insert box
/gate/crystal/geometry/setXLength 0.95 cm
/gate/crystal/geometry/setYLength 38.1 cm
/gate/crystal/geometry/setZLength 50.8 cm
/gate/crystal/placement/setTranslation 0.675 0. 0. cm
/gate/crystal/setMaterial NaI
/gate/crystal/vis/forceSolid
/gate/crystal/vis/setColor yellow
```

```
# BACK-COMPARTMENT
# Create the back-compartment volume
##
/gate/SPECThead/daughters/name compartment
/gate/SPECThead/daughters/insert box
/gate/compartment/geometry/setXLength 2.5 cm
/gate/compartment/geometry/setYLength 38.1 cm
/gate/compartment/geometry/setZLength 50.8 cm
/gate/compartment/placement/setTranslation 2.4 0. 0. cm
/gate/compartment/setMaterial Glass
/gate/compartment/vis/forceSolid
/gate/compartment/vis/setColor grey
# Repeat the head detector
# Move the detector
#/gate/SPECThead/repeaters/insert ring
#/gate/SPECThead/ring/setRepeatNumber 4
#/gate/SPECThead/moves/insert orbiting
#/gate/SPECThead/orbiting/setSpeed 30 deg/s
#/gate/SPECThead/orbiting/setPoint1 0 0 0 cm
#/gate/SPECThead/orbiting/setPoint2 0 0 1 cm
# TABLE
# Create the table volume
#/gate/world/daughters/name table
#/gate/world/daughters/insert box
#/gate/table/geometry/setXLength 25. cm
#/gate/table/geometry/setYLength 1.5 cm
#/gate/table/geometry/setZLength 160. cm
#/gate/table/placement/setTranslation 0. -5.75 0. cm
#/gate/table/setMaterial Glass
#/gate/table/vis/forceSolid
#/gate/table/vis/setColor white
```



```
# sacici ortam
/gate/world/daughters/name scatter
/gate/world/daughters/insert box
/gate/scatter/geometry/setXLength 15. cm
/gate/scatter/geometry/setYLength 30. cm
/gate/scatter/geometry/setZLength 24. cm
/gate/scatter/placement/setTranslation -11.5 0. 0. cm
/gate/scatter/setMaterial Plastic
/gate/scatter/vis/forceWireframe
/gate/scatter/vis/setColor blue
# Phantom
/gate/scatter/daughters/name Phantom
/gate/scatter/daughters/insert cylinder
/gate/Phantom/geometry/setRmax 3. mm
/gate/Phantom/geometry/setRmin 0.5 mm
/gate/Phantom/geometry/setHeight 24. cm
/gate/Phantom/placement/setTranslation -2.5 5. 0. cm
/gate/Phantom/setMaterial Glass
/gate/Phantom/vis/forceSolid
/gate/Phantom/vis/setColor magenta

/gate/scatter/daughters/name Phantom2
/gate/scatter/daughters/insert cylinder
/gate/Phantom2/geometry/setRmax 3. mm
/gate/Phantom2/geometry/setRmin 0.5 mm
/gate/Phantom2/geometry/setHeight 24. cm
/gate/Phantom2/placement/setTranslation -2.5 -5. 0. cm
/gate/Phantom2/setMaterial Glass
/gate/Phantom2/vis/forceSolid
/gate/Phantom2/vis/setColor magenta
##
/gate/systems/SPECThead/crystal/attach crystal
/gate/systems/SPECThead/describe
```

```
crystal SD
##
/gate/crystal/attachCrystalSD
# Phantom SD
/attachPhantomSD
# P H Y S I C S
#####
/gate/physics/addProcess PhotoElectric
/gate/physics/processes/PhotoElectric/setModel StandardModel
/gate/physics/addProcess Compton
/gate/physics/processes/Compton/setModel PenelopeModel
/gate/physics/addProcess RayleighScattering
/gate/physics/processes/RayleighScattering/setModel
PenelopeModel
/gate/physics/addProcess ElectronIonisation
/gate/physics/processes/ElectronIonisation/setModel
StandardModel e-
/gate/physics/addProcess Bremsstrahlung
/gate/physics/processes/Bremsstrahlung/setModel StandardModele-
/gate/physics/addProcess MultipleScattering e-
/gate/physics/processList Enabled
/gate/physics/processList Initialized
# C U T S
#####
# Cuts for particle in WORLD
##
/gate/physics/Gamma/SetCutInRegion      SPECThead 0.1 cm
/gate/physics/Electron/SetCutInRegion   SPECThead 1.0 cm
# I N I T I A L I Z A T I O N
#####
/gate/run/initialize
/control/execute MoveVisu.mac
```

```
# D E F I N E   T H E   S O U R C E
#####
/gate/source/addSource SourceConfinement
/gate/source/SourceConfinement/gps/type Volume
/gate/source/SourceConfinement/gps/shape Cylinder
/gate/source/SourceConfinement/gps/radius .5 mm
/gate/source/SourceConfinement/gps/halfz 12. cm
/gate/source/SourceConfinement/gps/centre -14. 5. 0. cm
/gate/source/SourceConfinement/gps/particle gamma
/gate/source/SourceConfinement/gps/energy 140. keV
/gate/source/SourceConfinement/setActivity 100000000. Bq
/gate/source/SourceConfinement/gps/angtype iso
/gate/source/addSource SourceConfinement2
/gate/source/SourceConfinement2/gps/type Volume
/gate/source/SourceConfinement2/gps/shape Cylinder
/gate/source/SourceConfinement2/gps/radius .5 mm
/gate/source/SourceConfinement2/gps/halfz 12. cm
/gate/source/SourceConfinement2/gps/centre -14. -5. 0. cm
/gate/source/SourceConfinement2/gps/particle gamma
/gate/source/SourceConfinement2/gps/energy 140. keV
/gate/source/SourceConfinement2/setActivity 100000000. Bq
/gate/source/SourceConfinement2/gps/angtype iso
# D I G I T I Z E R
#####
/gate/digitizer/Singles/insert adder
/gate/digitizer/Singles/insert blurring
/gate/digitizer/Singles/blurring/setResolution 0.09695
/gate/digitizer/Singles/blurring/setEnergyOfReference 140. keV
/gate/digitizer/Singles/insert spblurring
/gate/digitizer/Singles/spblurring/setSpresolution 3. mm
/gate/digitizer/Singles/spblurring/verbose 0
/gate/digitizer/Singles/insert thresholder
/gate/digitizer/Singles/thresholder/setThreshold 126. keV
/gate/digitizer/Singles/insert upholder
/gate/digitizer/Singles/upholder/setUphold 154. keV
```

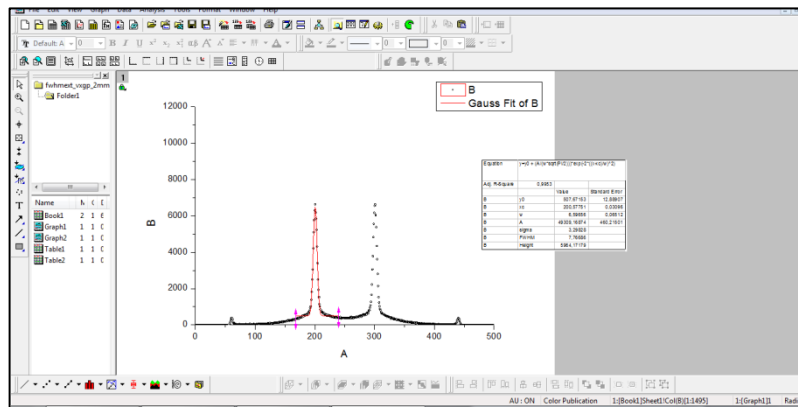
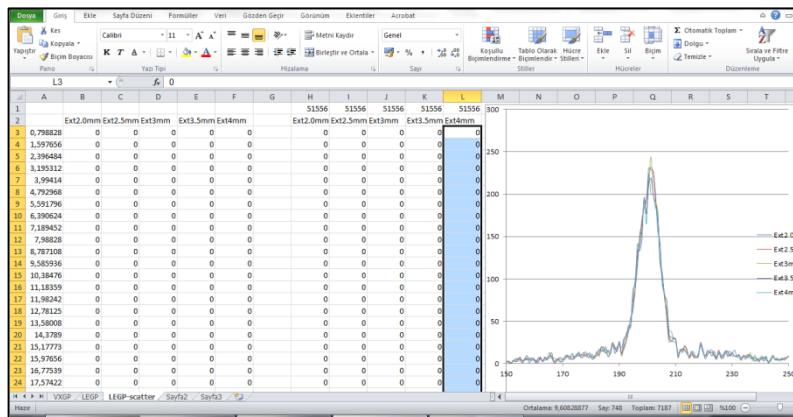
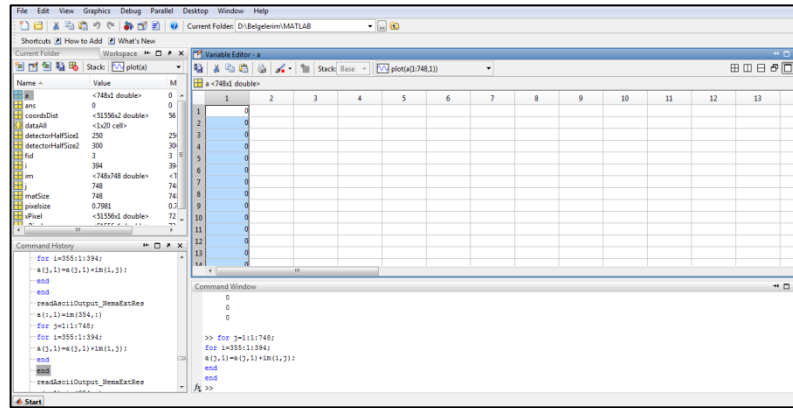
```

# O U T P U T
#####
#/gate/output/root/enable
#/gate/output/root/setFileName LineSourceX_DigRes4mm
#/gate/output/root/setRootHitFlag 1
#/gate/output/root/setRootSinglesAdderFlag 1
#/gate/output/root/setRootSinglesBlurringFlag 1
#/gate/output/root/setRootSinglesSpblurringFlag 1
#/gate/output/root/setRootSinglesThresholderFlag 1
#/gate/output/root/setRootSinglesUpholderFlag 1
/gate/output/ascii/enable
/gate/output/ascii/setFileName
ExtRes_VXGPscatter_Dig30En9695W126_154
/gate/output/ascii/setOutFileSinglesAdderFlag 1
/gate/output/ascii/setOutFileSinglesSpblurringFlag 1
/gate/output/ascii/setOutFileSinglesBlurringFlag 1
/gate/output/ascii/setOutFileSinglesThresholderFlag 1
/gate/output/ascii/setOutFileSinglesUpholderFlag 1
#   R A N D O M
# JamesRandom Ranlux64 MersenneTwister
/gate/random/setEngineName MersenneTwister
#/gate/random/setEngineSeed default
#/gate/random/setEngineSeed auto
/gate/random/setEngineSeed 123456789
#/gate/random/resetEngineFrom fileName
/gate/random/verbose 1
# P R O J E C T I O N
#####
#/gate/output/projection/enable
#/gate/output/projection/setFileName proj
/gate/output/projection/pixelSizeX 0.5 mm
/gate/output/projection/pixelSizeY 0.5 mm
/gate/output/projection/pixelNumberX 128
/gate/output/projection/pixelNumberY 128
# Specify the projection plane (XY, YZ or ZX)
##
/gate/output/projection/projectionPlane YZ

```

```
# E X P E R I M E N T
#####
/gate/application/setTimeSlice      1 s
/gate/application/setTimeStart      0 s
/gate/application/setTimeStop       6 s
```

## APPENDIX F :IMAGING OF PRO-ORGIN AND MATLAB



## **SIMULATION OF GAMMA CAMERA IN YEDITEPE UNIVERSITY HOSPITAL WITH GATE**

Gülçin İrim

Physics Department M.S. Thesis, 2013

Thesis Supervisor: Assoc. Prof. Ş. İpek KARAASLAN

The aim of this thesis is to have a detail simulation of Gamma Camera in Yeditepe University Hospital Nuclear Medicine Deapartment to carry the personal dosimetric calculations for all the patients before the treatment.

In this thesis, Gamma Camera being used routinely in Yeditepe University Hospital Nuclear Mecidine Department was investigated experimentally and with Monte Carlo simulation. A new and open Monte Carlo Code source, GATE, was used that for simulations running commands in C++ language.

Keywords: Gamma Camera, Monte Carlo Code, GATE, simulation, NEMA acceptance tests